

FGF and canonical Wnt signaling cooperate to induce paraxial mesoderm from tailbud neuromesodermal progenitors through regulation of a two-step epithelial to mesenchymal transition

Hana Goto, Samuel C. Kimmey, Richard H. Row, David Q. Matus and Benjamin L. Martin*

ABSTRACT

Mesoderm induction begins during gastrulation. Recent evidence from several vertebrate species indicates that mesoderm induction continues after gastrulation in neuromesodermal progenitors (NMPs) within the posteriormost embryonic structure, the tailbud. It is unclear to what extent the molecular mechanisms of mesoderm induction are conserved between gastrula and post-gastrula stages of development. Fibroblast growth factor (FGF) signaling is required for mesoderm induction during gastrulation through positive transcriptional regulation of the T-box transcription factor *brachyury*. We find in zebrafish that FGF is continuously required for paraxial mesoderm (PM) induction in post-gastrula NMPs. FGF signaling represses the NMP markers *brachyury* (*ntla*) and *sox2* through regulation of *tbx16* and *magn1*, thereby committing cells to a PM fate. FGF-mediated PM induction in NMPs functions in tight coordination with canonical Wnt signaling during the epithelial to mesenchymal transition (EMT) from NMP to mesodermal progenitor. Wnt signaling initiates EMT, whereas FGF signaling terminates this event. Our results indicate that germ layer induction in the zebrafish tailbud is not a simple continuation of gastrulation events.

KEY WORDS: EMT, FGF, Wnt, Neuromesodermal progenitor, Tailbud, Zebrafish

INTRODUCTION

The mesodermal germ layer is the origin of essential elements of the adult body such as the musculoskeletal, cardiovascular, renal and reproductive systems. Although a large bulk of the mesodermal germ layer is specified during gastrulation, accumulating evidence across multiple vertebrate species indicates that mesoderm induction continues after gastrulation in a population of neuromesodermal progenitors (NMPs) in the posteriormost embryonic structure, the tailbud (Beck, 2015; Henrique et al., 2015; Kimelman, 2016; Kimelman and Martin, 2012; Kondoh and Takemoto, 2012; Martin, 2016). All vertebrate embryos form their bodies in an anterior to posterior progression, and the tailbud NMPs are an essential source of new neural and mesodermal cells that contribute to the posteriorly elongating body axis (Beck, 2015; Henrique et al., 2015; Kimelman, 2016; Kimelman and Martin, 2012; Kondoh and Takemoto, 2012; Martin, 2016). While the molecular mechanisms of mesoderm induction during gastrulation are well studied, much less is known about how mesoderm is induced in NMPs


(Kiecker et al., 2016; Kimelman, 2006; Martin, 2016). Investigating this process will provide insight into the plasticity of mesoderm induction programs and strengthen our understanding of how the vertebrate body plan is established.

The first mesoderm-inducing signal discovered was the fibroblast growth factor (FGF) pathway (Dorey and Amaya, 2010; Kiecker et al., 2016). When overexpressed, FGF signaling is sufficient to induce mesoderm in naïve epiblast cells (Kimelman et al., 1988; Kimelman and Kirschner, 1987; Slack et al., 1987). Additionally, loss of FGF signaling across many vertebrate species results in defects in gastrula stage paraxial mesoderm (PM) induction (Amaya et al., 1991; Deng et al., 1994; Griffin et al., 1995; Mitrani et al., 1990; Yamaguchi et al., 1994). A conserved downstream transcriptional target of FGF signaling is the T-box transcription factor *brachyury* (Latinkic et al., 1997), which itself has a conserved role in mesoderm formation through canonical Wnt signaling regulation (Martin and Kimelman, 2008, 2009). Loss of early FGF signaling causes a loss of *brachyury* expression, leading to defects in mesoderm induction (Ciruna and Rossant, 2001; Griffin et al., 1995; Isaacs et al., 1994; Latinkic et al., 1997). FGF signaling continues to be active in the tailbud, where it plays crucial roles in maintaining the progenitors of the spinal cord (called the neural stem zone), in promoting the proper migration of cells through the tailbud and PM, and in establishing wavefront activity necessary for somitogenesis, although its role in tailbud mesoderm induction from NMPs is unknown (Akai et al., 2005; Dubrulle et al., 2001; Hubaud and Pourquie, 2014; Lawton et al., 2013; Mathis et al., 2001; Steventon et al., 2016). By contrast, canonical Wnt signaling is known to have a conserved essential role during the induction of mesoderm from NMPs (Bouldin et al., 2015; Garriock et al., 2015; Gouti et al., 2014; Henrique et al., 2015; Jurberg et al., 2014; Martin and Kimelman, 2012; Tsakiridis et al., 2014; Wymeersch et al., 2016). In the absence of Wnt signaling, NMPs fail to become mesoderm and instead give rise to the spinal cord.

The formation of mesoderm during gastrulation requires an epithelial to mesenchymal transition (EMT) as cells move from the epithelial epiblast to the mesenchymal mesoderm (Acloque et al., 2009). Several mesoderm-inducing signaling pathways, including canonical Wnt, TGF β and FGF, promote the gastrula stage mesodermal EMT (Acloque et al., 2009). The study of post-gastrula EMT in NMPs has been hampered by the lack of tailbud-specific EMT molecular markers, and has been limited to analysis of cell behaviors in the tailbud (Lawton et al., 2013; Manning and Kimelman, 2015; Steventon et al., 2016). After gastrulation, cells exhibit behavioral changes as they transition from NMP to PM. NMPs exhibit collective epithelial-like migration, whereas the mesoderm derived from NMPs exhibits rapid individual cell migration consistent with mesenchyme (Lawton et al., 2013). In zebrafish, the mesodermal EMT during both gastrulation and

Department of Biochemistry and Cell Biology, Stony Brook University, Stony Brook, NY 11794-5215, USA.

*Author for correspondence (benjamin.martin@stonybrook.edu)

 B.L.M., 0000-0001-5474-4492

Received 15 August 2016; Accepted 16 February 2017

later in the tailbud occurs as a two-step process (Manning and Kimelman, 2015; Row et al., 2011). In the first step, cells initially transition from epithelium to non-directionally migrating mesenchyme, followed by a second EMT completion step, in which cells transition from non-directional to directional migration. The transcription factors *Tbx16* and *Msgn1* are essential for promoting the second step of the EMT, and in their absence cells become stuck in the intermediate state and fail to develop into PM (Manning and Kimelman, 2015; Row et al., 2011).

We identified new molecular markers of EMT in zebrafish and performed high-resolution imaging of tailbud cells undergoing EMT. These new tools were used in combination with reagents to temporally manipulate signaling pathways and gene activity to examine FGF regulation of tailbud mesoderm induction. We find that FGF cooperates with Wnt signaling to induce PM from NMPs during a two-step EMT event. Wnt signaling initiates the EMT, and FGF signaling terminates this event. Together, our results shed light on the molecular control of a two-step EMT, as well as highlighting previously unrecognized differences in the mechanisms of mesoderm induction between gastrula and post-gastrula stages of development.

RESULTS

FGF signaling is required for PM induction from NMPs

To determine whether FGF signaling continues to be required for mesoderm induction in the tailbud, we used a heat shock-inducible dominant-negative FGF receptor transgenic line to temporally inhibit FGF signaling (*HS:dnfgfr1-gfp*; hereafter abbreviated as *HS:dnfgfr1*) (Lee et al., 2005). Loss of FGF signaling at the 12- or 18-somite stage resulted in a significant deficit in the generation of posterior somitic mesoderm, as indicated by a loss of posterior somites (Fig. 1A-E). Posterior notochord, which is formed from separate populations of plastic progenitor cells (Row et al., 2016), is relatively unaffected after loss of FGF signaling (Fig. 1F-I). The undulating notochord in FGF loss-of-function embryos indicates expansion of notochord despite the failure of the tail to continue to extend. These results imply that FGF signaling is required for post-gastrula PM induction specifically in the posterior wall NMPs (in the posteriormost domain of the tailbud) that generate the somites, and not the midline NMPs that form notochord (Row et al., 2016).

During gastrula stage mesoderm induction, FGF signaling is required to activate and maintain *brachyury* expression (Amaya et al., 1993; Delaune et al., 2005; Fletcher and Harland, 2008; Griffin et al., 1995; Isaacs et al., 1994; Schulte-Merker and Smith, 1995). We confirmed that loss of FGF signaling using the *HS:dnfgfr1* line during gastrulation resulted in near complete loss of *T. brachyury homolog a* (*ta*; referred to here by the synonym *ntla*) expression (Fig. 1J,K). Loss of FGF signaling after gastrulation at the 8-somite stage resulted in the opposite effect – an expansion of *ntla* expression in the posterior tailbud (Fig. 1L,M). Tailbud NMPs are characterized by the co-expression of *ntla* and *sox2* (Martin and Kimelman, 2012; Olivera-Martinez et al., 2012). Similar to *ntla*, *sox2* expression in the tailbud was expanded after loss of FGF signaling (Fig. 1N,O). These results suggest that the role of FGF signaling during mesoderm induction in the tailbud differs mechanistically from its role during gastrulation, and that in the tailbud FGF signaling is required to repress NMP markers *ntla* and *sox2* to promote PM differentiation.

Two new *vimentin*-related genes are expressed specifically in tailbud cells undergoing EMT

The expansion of *ntla* in the tailbud after loss of FGF signaling is reminiscent of embryos that are mutant for *tbx16* (also known as

spadetail). Homozygous *tbx16* mutants exhibit greatly expanded *ntla* expression in the tailbud (Fior et al., 2012; Yabe and Takada, 2012). During tailbud mesoderm induction from NMPs, future mesodermal cells undergo a two-step EMT (Manning and Kimelman, 2015). In the first step, cells go from an epithelial-like to a mesenchymal state without directional movement. In the second step, non-directional mesenchyme acquires directional movement and cells exit the tailbud. The second step is dependent on *Tbx16* and *Msgn1* function; they promote exit from the tailbud as well as repression of *ntla* expression (Bouldin et al., 2015; Fior et al., 2012; Manning and Kimelman, 2015; Row et al., 2011). Based on the similarity in phenotype, we reasoned that loss of FGF signaling might specifically affect the ability to complete the second step of the EMT process.

There is currently a lack of characterized molecular EMT markers in the zebrafish tailbud. Expression of the intermediate filament vimentin is routinely used as a marker of cells undergoing EMT, but the expression pattern of a zebrafish *vimentin* ortholog is absent from the tailbud (Cerdà et al., 1998; Lowery et al., 2015; Ye and Weinberg, 2015). To determine whether zebrafish has other *vimentin* genes that are expressed in the tailbud, we searched the genome and found two additional *vimentin*-related genes. We named these genes (with approval from the Zebrafish Nomenclature Committee) *vimentin-related 1* (*vimr1* – currently annotated as CABZ01079764) and *vimentin-related 2* (*vimr2* – currently annotated as *si:dkey-76i15.1*). Both genes are expressed in the ventral tailbud precisely where new mesoderm is being generated from NMPs (Fig. 2A,B; Fig. S1). An amino acid alignment of *Vimr1* and *Vimr2* with vimentin proteins from other species indicates that *Vimr1* and *Vimr2* contain all of the conserved functional vimentin domains (Fig. 2C,E). Additionally, a phylogenetic analysis of vertebrate vimentin proteins and the closely related desmin intermediate filament proteins indicates that *Vimr1* and *Vimr2* cluster with vimentin proteins (Fig. 2D; Fig. S2). To determine whether *vimr1* and *vimr2* expression is specifically localized to cells undergoing EMT, we examined their expression in *tbx16* mutant embryos, in which tailbud cells are trapped in the intermediate EMT process. Both genes showed a dramatic expansion in *tbx16* mutants, suggesting that they are indeed specific to tailbud mesoderm undergoing EMT (Fig. 2F-I).

FGF signaling promotes completion of tailbud mesodermal EMT and mesoderm exit from the tailbud

To investigate whether FGF regulates EMT in the tailbud, we conducted *in situ* hybridization using the *vimr1* and *vimr2* markers in *HS:dnfgfr1* and in heat shock-inducible constitutively active *fgfr1* (*HS:cafgr1*) embryos. We find that inhibition of FGF signaling leads to expansion of *vimr1* and *vimr2* expression in the tailbud (Fig. 3A-D), whereas overactivation of FGF results in the reduction of *vimentin*-related gene expression (Fig. 3E-H; Fig. S3). These results suggest that FGF regulates the completion of EMT in tailbud mesodermal progenitors.

Since loss of FGF signaling in the tailbud produces a phenotype similar to loss of *tbx16* and *msgn1* function, and FGF regulates *tbx16* expression during gastrulation, we examined whether FGF signaling activates *tbx16* and *msgn1* expression in the tailbud (Griffin et al., 1998). Loss of FGF signaling resulted in a reduction of both *tbx16* and *msgn1*, particularly in the posteriormost domain where new cells are joining the PM (Fig. 3I-L', white arrowheads). The regulation of *msgn1* in the tailbud by FGF signaling has also been demonstrated previously (Fior et al., 2012). Gain of FGF function had the opposite effect, again most notably in the

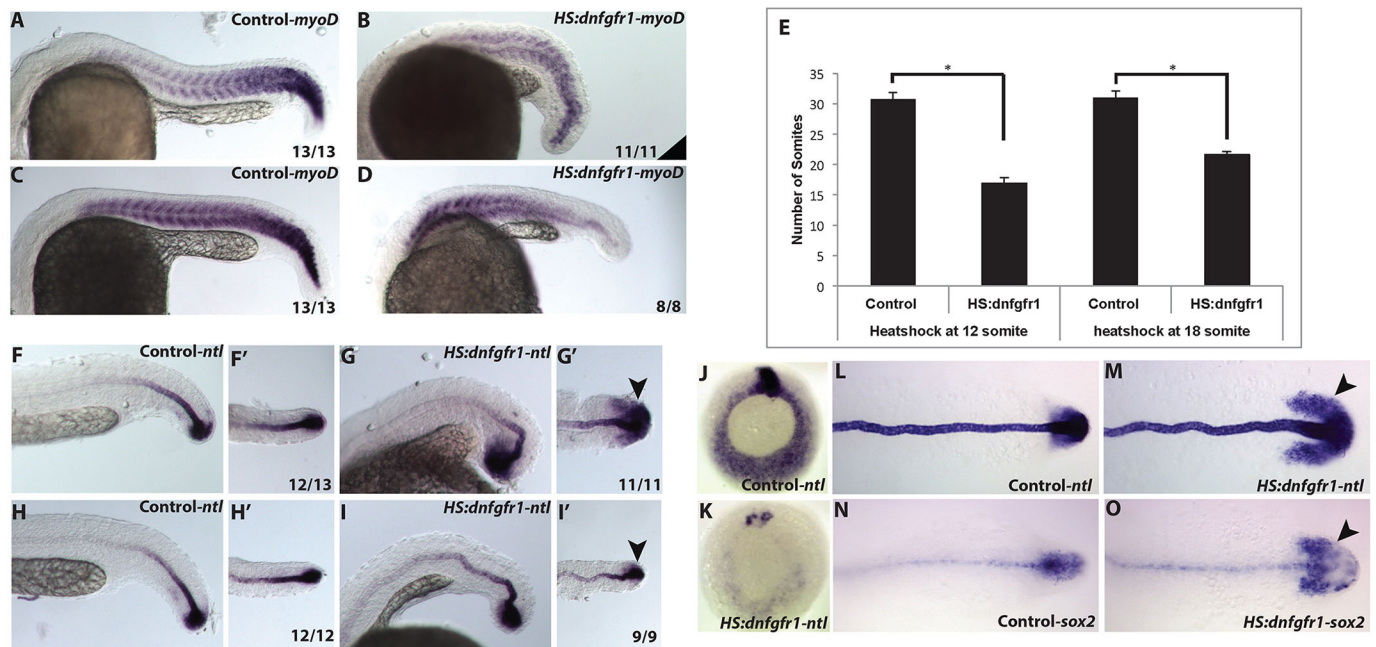


Fig. 1. FGF is required for post-gastrula mesoderm induction and repression of the NMP state. (A-E) Zebrafish embryos from an *HS:dnfgfr1* hemizygous outcross were heat shocked at the 12- or 18-somite stage and analyzed for *myoD* expression at 24 hpf. Wild-type siblings exhibit ~31 somites (A,C,E), whereas *HS:dnfgfr1* embryos heat shocked at 12 somites have 16 somites and those heat shocked at 18 somites have 22 somites (B,D,E). The number of embryos showing the illustrated phenotype among the total number examined is indicated. Error bars indicate s.d. * $P < 0.001$ (using unpaired *t*-test). (F-I') Expression of *ntla* (arrowheads) indicates that there is no posterior loss of notochord after FGF inhibition at the 12- or 18-somite stage. (J,K) Embryos heat shocked at 50% epiboly (just at the start of gastrulation) and fixed 3 h after heat shock show a near complete loss of *ntla* expression. (L,M) Embryos heat shocked at the 8-somite stage and fixed 3 h later exhibit an expansion of *ntla* into lateral and anterior domains (arrowhead). (N,O) Inhibition of FGF signaling at the 8-somite stage also leads to an expansion of *sox2* 3 h after the heat shock. (A-D,F,G,H,I) Lateral view, anterior left; (F',G',H',I',L-O) dorsal view, anterior left; (J,K) vegetal view, dorsal top.

posteriormost domain (Fig. 3M-P'). Co-staining for Tbx16 protein and *vimr1* mRNA showed a small region of *vimr1* overlap with the posteriormost domain of Tbx16 expression in wild-type embryos (Fig. 3Q-Q''; Fig. S3). This implies that mesodermal progenitors rapidly exit the EMT process upon Tbx16 expression. In embryos lacking FGF function, Tbx16 expression is reduced and there is a corresponding expansion of *vimr1* expression, suggesting that tailbud mesodermal progenitors are trapped in the intermediate EMT state owing to a lack of Tbx16 (and likely also *Msgn1*) expression (Fig. 3R-R'').

The expansion of *vimr1* and *vimr2* expression in the tailbud in *tbx16* mutant embryos and after loss of FGF signaling suggests that cells lacking FGF function fail to exit the tailbud and join somites, similar to *tbx16* mutant cells. To directly visualize the effect of FGF inhibition on the movement of mesodermal progenitors, we performed live quantitative imaging of wild-type, SU5402-treated wild-type, *HS:tbx16*, and SU5402-treated *HS:tbx16* tailbuds. Embryos were labeled with a nuclear-localized photoconvertible protein (*NLS-kikume*) and heat shocked at the 12-somite stage, followed by green to red photoconversion of small groups of cells along the posterior wall of the tailbud (where NMPs normally reside). These embryos were time-lapse imaged by spinning disc confocal microscopy (Fig. 4A-E; all conditions can be viewed in Movies 8-17). Control wild-type progenitors are able to undergo ventral diving and rapid displacement into the maturation zone, where they mix with each other (Fig. 4Aa-d'). By contrast, FGF-inhibited progenitor cells exhibited a delayed cell movement, which resulted in fewer cells moving into the maturation zone and the PM (Fig. 4Ca-d'). Cell nuclei were tracked using Imaris software (Fig. 4Fa-e, Ga-e) and tracks were quantified. Loss of FGF signaling

caused a significant decrease in mean displacement length and mean track speed compared with wild-type cells (Fig. 4I; Table S1). The forced expression of *tbx16* in FGF loss-of-function cells caused a statistically significant rescue of mean displacement length and mean track speed (Fig. 4H,I; Table S1). Track straightness remained largely unaffected in all treatment groups (Fig. 4J; Table S1). These results show that FGF is required for cell movement out of the tailbud, and that expression of Tbx16 is sufficient to rescue movement in the absence of FGF signaling.

To further confirm that *tbx16* and *msgn1* function downstream of FGF signaling to promote EMT termination, we performed epistasis experiments. Wild-type embryos, embryos from the *HS:tbx16* transgenic line, or embryos from an *HS:msgn1* transgenic line were treated with SU5402 (Fig. 5A-P) (Row et al., 2016). Heat shock induction of *tbx16* or *msgn1* alone caused complete loss of *vimr1* and *vimr2* expression in the tailbud, similar to activation of FGF signaling (Fig. 5C,G,K,O). The combined loss of FGF signaling and gain of *tbx16* or *msgn1* expression resulted in the complete absence of *vimr1* and *vimr2* expression, indicating rescue of the enhanced *vimr1* and *vimr2* expression seen with loss of FGF signaling alone (Fig. 5D,H,L,P). These results support a model in which FGF signaling promotes EMT completion and PM induction through positive regulation of *tbx16* and *msgn1* transcription.

To add support to this model, we performed mosaic epistasis analysis of NMPs that have changes in FGF signaling levels, *tbx16* or *msgn1* levels, or both FGF signaling and *tbx16* or *msgn1*, by transplanting cells with heat shock-inducible constructs into wild-type hosts. Cells from sphere stage donor embryos were transplanted into the ventral margin of unlabeled shield stage wild-type embryos, which is an established strategy for targeting donor cells to the NMP

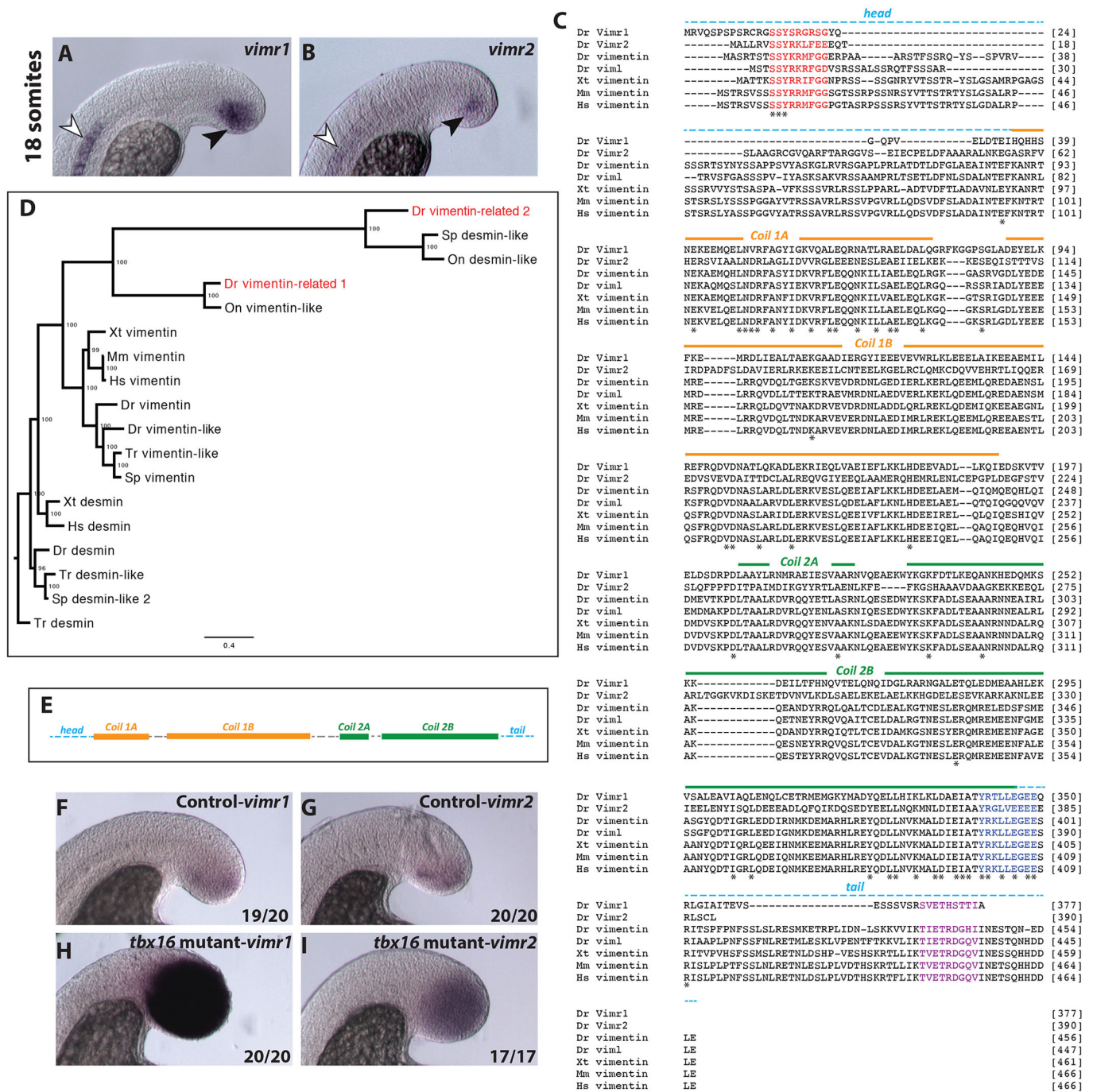


Fig. 2. Two vimentin-related genes, *vimr1* and *vimr2*, are expressed specifically in cells undergoing EMT in the tailbud. Expression pattern of *vimr1* (A) and *vimr2* (B) in wild-type 18-somite stage embryos. Expression of both genes is limited to the notochord and tailbud cells during somitogenesis (white arrowheads indicate notochord expression, black arrowheads tailbud expression). (C) Protein alignment derived from *vimentin* gene sequences. Red indicates a highly conserved motif, which has been shown to have a role in vimentin assembly (Herrmann et al., 1992); blue indicates the helix termination motif and purple indicates the beta site. Zebrafish sequences include that of another *vimentin* gene, *vimentin-like* (*viml*). (D) Bayesian phylogenetic analysis of *Vimr1* and *Vimr2* protein sequences with desmin proteins serving as an outgroup. Numbers at the node specify Bayesian posterior probabilities. Dr, *Danio rerio* (zebrafish); Hs, *Homo sapiens* (human); Mm, *Mus musculus* (mouse); On, *Oreochromis niloticus* (Nile tilapia); Sp, *Stegastes partitus* (bicolor damselfish); Tr, *Takifugu rubripes* (pufferfish); Xt, *Xenopus tropicalis* (frog). (E) Schematic of vimentin-related intermediate filament. Head and tail domains are indicated by dashed lines, whereas helix-rich regions of the rod domain are represented by filled boxes. (F-I) Expression of *vimr1* and *vimr2* in *tbx16* (*spt^{tb104}*) mutants (H,I) and their wild-type control siblings (F,G). (A,B,F-I) Lateral views of the posterior tailbud domain.

population (Martin and Kimelman, 2012). Host embryos were heat shocked at the bud stage and live imaged at 30 h post fertilization (hpf) and analyzed for whether the cells contribute to the somites (Fig. 5Q-U). The vast majority of cells that join zebrafish somites become skeletal muscle, the fate of which can be easily identified

by morphology and location (Fig. 5R). Approximately 70% of wild-type cells, *HS:tbx6* cells, or *HS:mgn1* cells transplanted into wild-type host embryos contribute to posterior somites in the form of skeletal muscle (Fig. 5V; Table S2). Transplanted cells lacking FGF signaling exhibit a significant reduction in somite contribution,

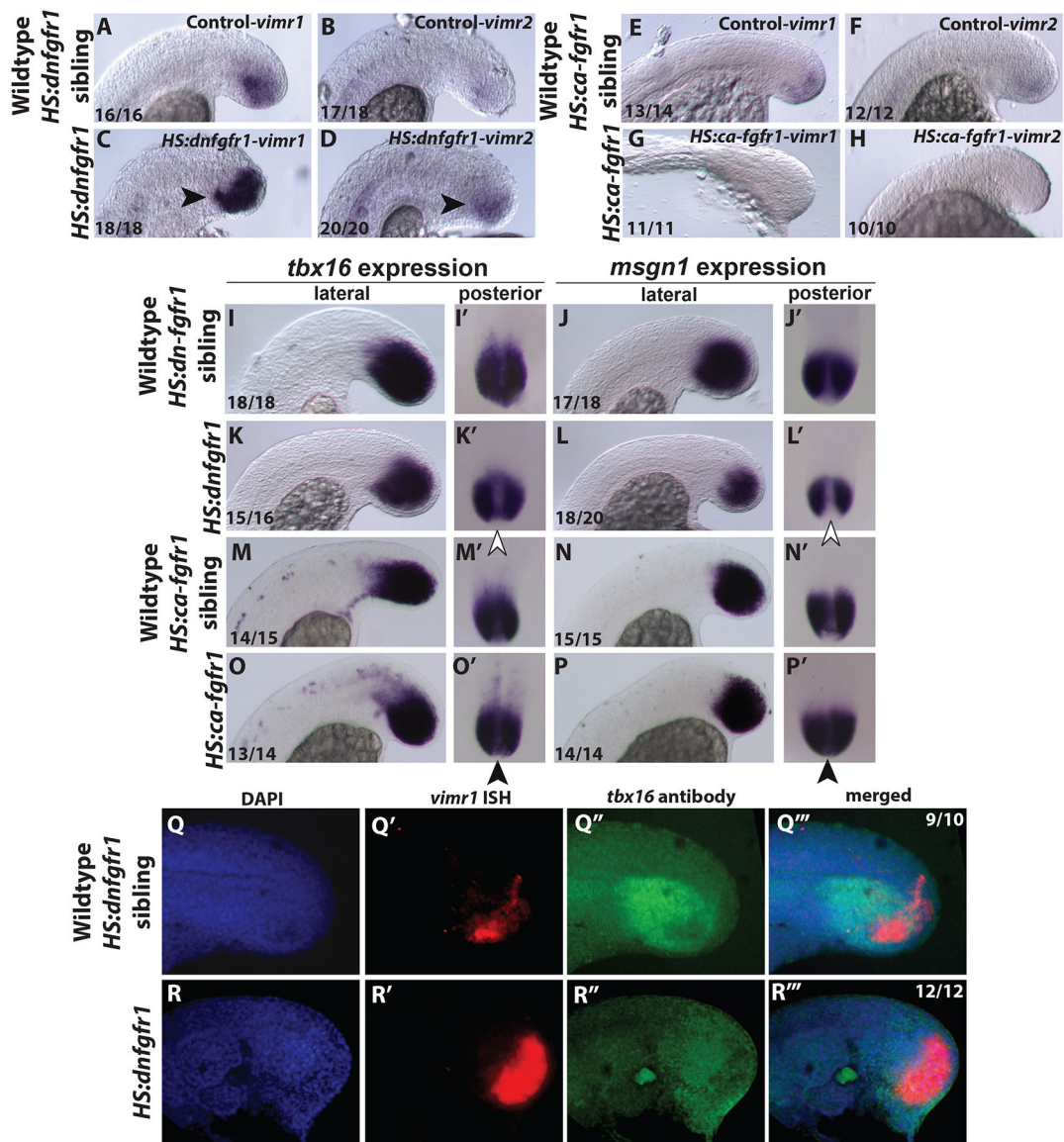


Fig. 3. FGF is required for EMT termination during tailbud mesoderm formation. (A-H) The expression of *vimr1* and *vimr2* was examined at the 20-somite stage in *HS:dmgfr1* embryos (C,D) and their wild-type siblings (A,B) that were heat shocked at the 12-somite stage, as well as in *HS:cafgfr1* embryos (G,H) and their wild-type siblings (E,F). Expression of *vimr1* and *vimr2* is increased in loss of FGF function embryos (C,D, arrowheads) and decreased in gain of FGF function embryos (G,H). (I-P) The expression of *tbx16* and *msgn1* decreases in FGF-inhibited tailbuds (K-L') as compared with sibling controls (I-J'). Conversely, expression of *tbx16* and *msgn1* increases in FGF-overactivation embryos (O-P') compared with their wild-type controls (M-N'). White arrowheads (K',L'; dorsal view) indicate loss of expression at the tip and midline of the tailbud. Black arrowheads (O',P'; dorsal view) indicate ectopic expression at the tip and midline of the tailbud. (Q-R'') Co-expression of *vimr1* and Tbx16 was examined in 20-somite stage wild-type (Q-Q'') and *HS:dmgfr1* (R-R'') embryos that were heat shocked at 12 somites. FGF inhibition increases the expression of *vimr1* while reducing the expression domain of Tbx16 (compare Q',Q'' with R',R''). All tailbud images are lateral views except where indicated.

which is down to 20%. The activation of *tbx16* or *msgn1* in FGF loss-of-function cells results in a significant rescue of somite muscle contribution (Fig. 5V). These results suggest that an essential role of FGF signaling during PM induction from NMPs is to activate transcription of *tbx16* and *msgn1*.

An essential role of Tbx16 and Msgn1 during NMP mesoderm specification is the transcriptional repression of the NMP markers *ntla* and *sox2* (Bouldin et al., 2015; Fior et al., 2012). We demonstrated that loss of FGF signaling at the 8-somite stage results in the expansion of *ntla* and *sox2* expression. To demonstrate that transplanted cells lacking FGF signaling also fail to repress *ntla* and *sox2* expression, we transplanted *HS:dmgfr1* cells into the ventral margin of wild-type host embryos, heat shocked them at the 8-somite

stage, and fixed them at the 12-somite stage (Fig. 5W-AAf). In hosts containing transplanted wild-type cells, ectopic *ntla* or *sox2* expression was never observed (Fig. 5Xa-f,Za-f). By contrast, host embryos containing transplanted *HS:dmgfr1* cells exhibited punctate ectopic expression of *ntla* and *sox2* in the posterior of the embryo (Fig. 5Ya-f,AAa-f). These results imply that cells lacking FGF signaling fail to join the PM owing to their inability to repress the NMP state and to progress into a PM program.

FGF signaling cooperates with Wnt signaling for the continuous generation of new PM from the NMP population

Previous work has shown that transplanted cells lacking Wnt signaling in the NMP population fail to become mesoderm but,

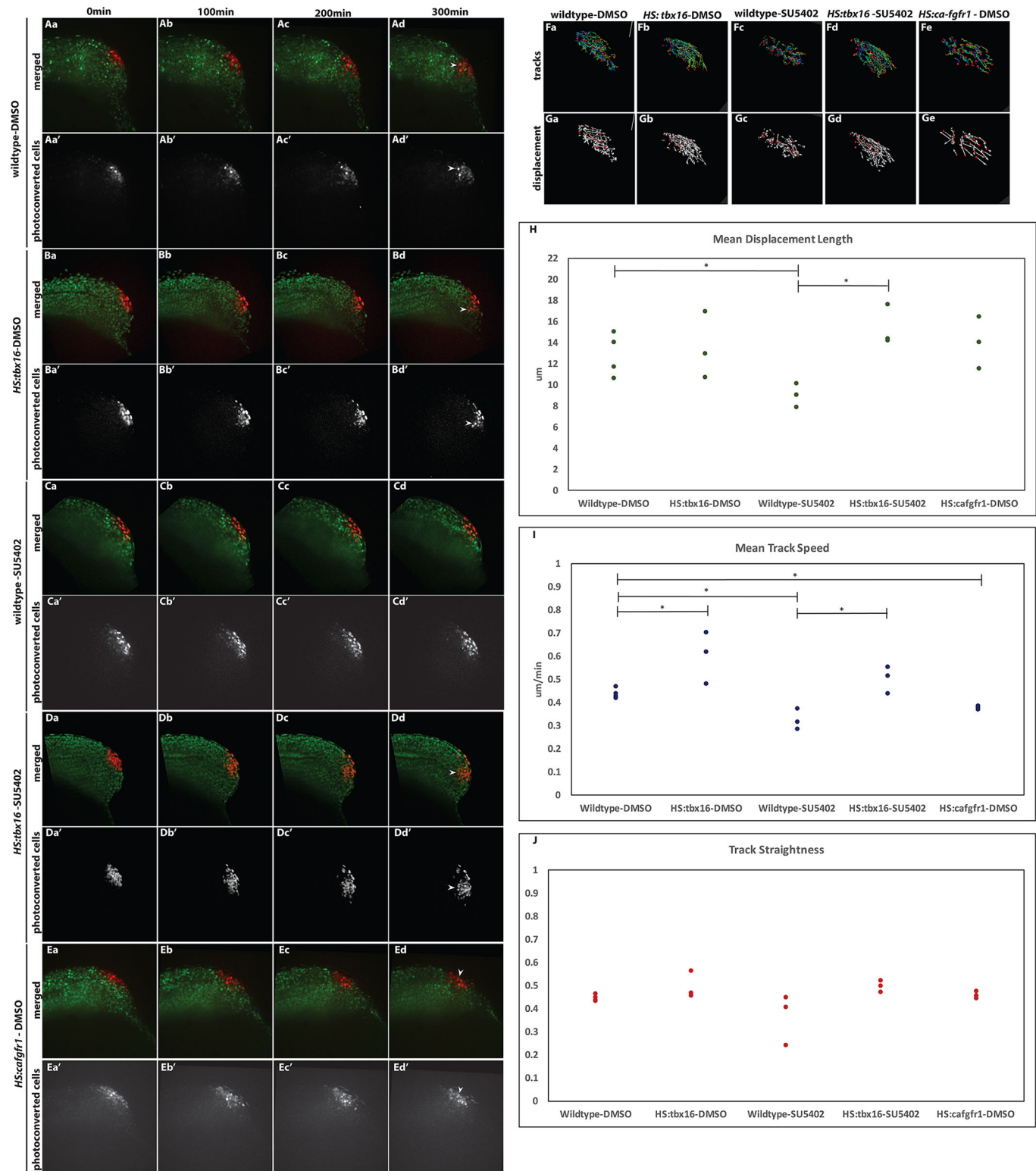


Fig. 4. FGF regulates tailbud cell displacement through *tbx16* regulation. (A-E) Time-lapse images of photoconverted tailbud cells of *NLS-kikume* mRNA-injected wild-type cells (Aa-d', Ca-d'), *HS:tbx16* (Ba-d', Da-d') and *HS:cafgfr1* (Ea-d') embryos at 12-somite stage and onward, as indicated. DMSO-treated wild-type cells were able to move rapidly from the progenitor zone (Aa-d'), whereas SU5402-treated wild-type cells remained within the tailbud (Ca-d'). Activation of *tbx16* rescues cell displacement and speed in the presence of SU5402 (Da-d'). Cells with activated FGF signaling also enter the maturation zone similarly to wild-type embryos (Ea-d' versus Aa-d'), but not as rapidly as *tbx16*-overexpressing cells (Ba-d'). White arrowheads point to cells entering the maturation zone. (F,G) Tracking of photoconverted cells as shown in trajectories (Fa-e) and displacement vector (Ga-e). (H-J) The mean displacement, mean track speed and mean track straightness of photoconverted cells. The mean displacement and the speed decrease in SU5402-treated wild-type embryos compared with vehicle-treated wild-type embryos (H versus I). *tbx16* overexpression rescues the displacement and speed in SU5402-treated embryos. Track straightness did not differ significantly among the treatment groups (J). * $P < 0.05$, unpaired two-way *t*-tests.

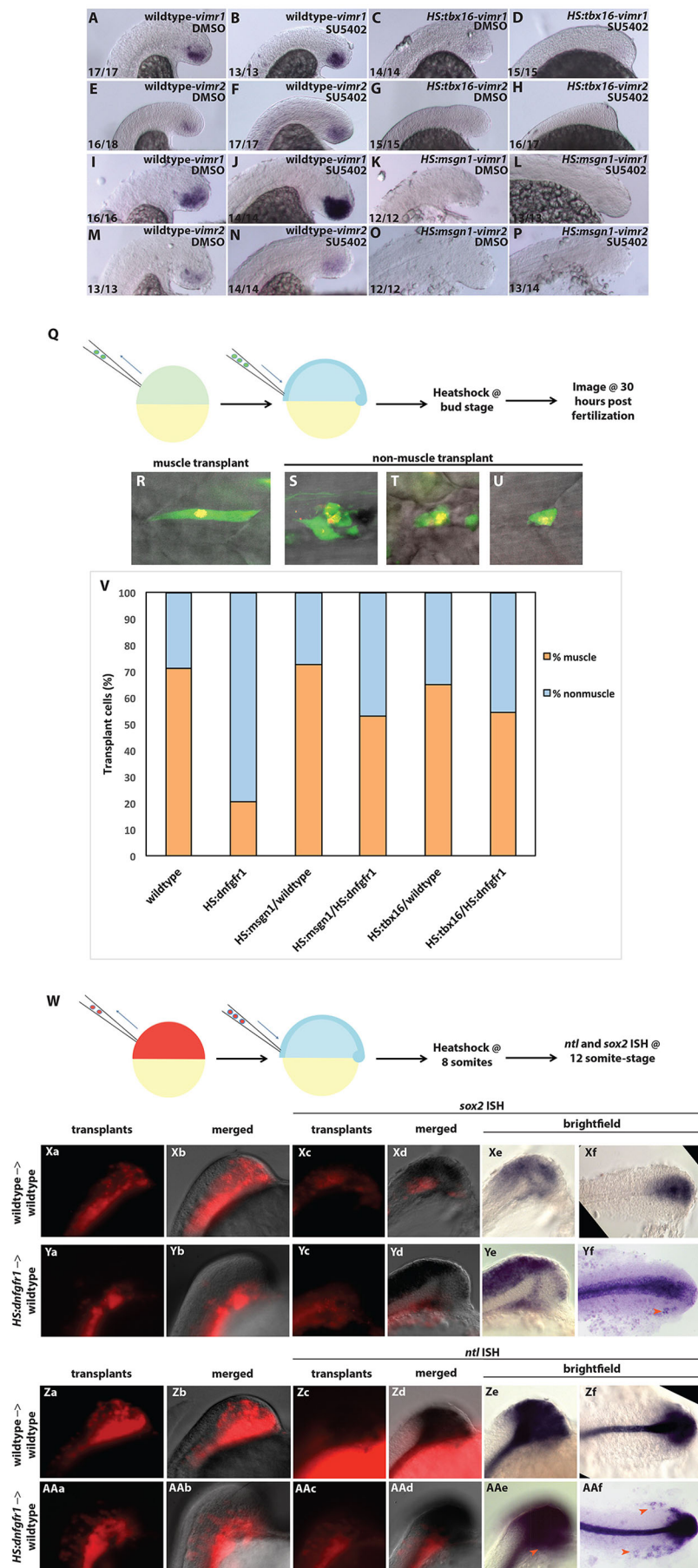


Fig. 5. FGF promotes mesoderm induction and inhibition of the NMP state via *tbx16* and *msgn1*. (A-P) Expression of *vimr1* and *vimr2* was analyzed in SU5402- or DMSO-treated *HS:tbx16*, *HS:msgn1* and wild-type sibling control embryos. Embryos were heat shocked at the 12-somite stage and analyzed at the 20-somite stage. Activation of *tbx16* eliminates *vimr1* and *vimr2* expression in DMSO-treated (C,G) and SU5402-treated (compare D,H with B,F) embryos. Similarly, *msgn1* activation inhibits *vimr1/2* expression in DMSO-treated (K,O) and SU5402-treated (compare L,P with J,N) embryos. (Q-V) A transplant assay was used in epistasis experiments to determine whether *tbx16* and *msgn1* function downstream of FGF during termination and if these genes could rescue somite fate of FGF-inhibited tailbud cells. Wild-type donor embryos were injected with a mixture of fluorescein-dextran and heat shock-inducible *HS:tbx16*, *HS:msgn1* or control *HS:NLS-kikume* plasmids. At sphere stage, the cells from these donor embryos were transplanted into the ventral margin of unlabeled wild-type shield stage host embryos, which targets them to the NMP population (Q). Embryos were heat shocked at the bud stage and examined at 30 hpf. The kikume protein was photoconverted prior to imaging and the lineage analysis was performed based on cell shapes and location of the transplanted cells. The majority of the transplanted wild-type cells contribute to somites, as do cells with *tbx16* and *msgn1* overexpression (R,V). The majority of the transplanted *HS:dnfgr1* cells are excluded from somites and do not form muscle (S-V) and remain in the tail region. However, upon the presence of *tbx16* or *msgn1*, FGF-inhibited cells contribute to somites and form skeletal muscle (V). (W-AAf) A similar assay was used to determine whether transplanted cells that lack FGF function cell-autonomously maintain NMP markers *sox2* and *ntla* (W). Host embryos containing transplanted wild-type cells and stained for *sox2* (Xa-f) or *ntla* (Za-f) exhibit normal *sox2* and *ntla* expression patterns, whereas host embryos with *HS:dnfgr1* cells have ectopic *sox2* (Ya-f) and *ntla* (AAa-f) expressing cells in the tailbud (red arrowheads). Xa-e, Ya-e, Za-e, AAa-e, lateral views, anterior bottom; Xf, Yf, Zf, AAf, dorsal views, anterior left.

unlike cells lacking FGF signaling, these cells translocate to neural ectoderm (Martin and Kimelman, 2012). With respect to the two-step mesodermal EMT, this suggests that Wnt signaling initiates the EMT, whereas FGF signaling terminates it, allowing cells to join the PM. In the presence of Wnt but absence of FGF, cells are trapped in the intermediate EMT state and fail to join the PM. To test this model with respect to *vimr1* and *vimr2* expression, we used the *HS:TCFΔC* transgenic line to inhibit Wnt signaling at the 12-somite stage and examined *vimr1* and *vimr2* expression 5 h after the heat shock. We observed a dose-dependent loss of *vimr1* and *vimr2* expression after Wnt loss of function, where one copy of the transgene caused a reduction of *vimr1* and *vimr2* expression compared with wild-type embryos, and two copies of the transgene resulted in near complete loss of *vimr1* and *vimr2* expression (Fig. 6A-F). Whereas *mshn1* expression was reduced in Wnt loss-of-function embryos, *tbx16* expression was unaffected (Fig. 6K-P'). These results show that Wnt signaling induces initiation of mesodermal EMT.

We next asked whether activation of Wnt signaling is sufficient to cause an accumulation of *vimr1*- and *vimr2*-expressing cells as a consequence of too many cells initiating the EMT event. Surprisingly, we found that activation of Wnt signaling using an *HS:caβ-catenin* transgenic line resulted in a loss rather than gain of *vimr1* and *vimr2* expression (Fig. 6G-J). We examined *tbx16* and *mshn1* expression in these embryos and found strong expansion of both genes upon Wnt activation (Fig. 6Q-T'). This implies that elevated Wnt signaling is sufficient to promote the second EMT exit step. To determine whether Wnt is sufficient to induce the completion of the EMT event in the absence of FGF signaling, we compared *vimr1* expression in embryos with activated Wnt signaling alone or with activation of Wnt and inhibition of FGF signaling using the small molecule FGF receptor inhibitor SU5402. Whereas activation of Wnt signaling led to a complete loss of *vimr1* expression within 5 h after the heat shock induction, it was unable to do so in the absence of FGF signaling. After simultaneous induction of β-catenin and inhibition of FGF receptor, *vimr1* expression was similar to, or slightly stronger than, that in wild-type embryos (Fig. 6U-X). Together, these results suggest that during PM induction from NMPs, Wnt signaling initiates the EMT event and FGF promotes the completion of EMT and exit into the PM.

High-resolution imaging of the tailbud EMT

In order to directly visualize the tailbud EMT process, we developed a new transgenic line that expresses membrane-localized mCherry and nuclear-localized kikume after heat shock induction [*HS:(CAAX)mCherry-p2a-(NLS)kikume*]. Cells from this stable transgenic line were transplanted into the ventral margin of unlabeled wild-type host embryos to target them to the NMP population. We observed that cells in the NMP domain of the posterior wall of the tailbud adhere to each other and to the border between the epidermis and the NMP population along the apical edge of the NMPs. In a process that appears strikingly similar to that described in a recent report of mouse epiblast cells undergoing EMT to form mesoderm during gastrulation (Ramkumar et al., 2016), individual cells were observed to undergo apical constriction, ingression, and epithelial layer exit, while remaining tethered to the epithelial layer by a long apical extension of the membrane for a period of time before complete dissociation (Fig. 7A,B, Movies 1 and 2). This process, as in the mouse, appears stochastic. After cells ingress from the epithelial layer, they exhibit rapid membrane protrusions (including lamellipodia, filopodia and blebs), before eventually migrating out of the tailbud, as previously observed

(Fig. 7G-I, Movies 4 and 5). We repeated these observations in transplanted cells lacking either Wnt signaling or FGF signaling, using the *HS:TCFΔC* or *HS:dnfgfr1* lines, respectively. Cells lacking Wnt signaling were unable to leave the NMP epithelial layer and remained in the posterior wall of the tailbud adjacent to the epidermis (Fig. 7E,F compared with C,D; Movie 3), whereas cells lacking FGF signaling appeared to leave the NMP epithelial layer normally. Like wild-type cells, after leaving the NMP layer the cells lacking FGF signaling exhibited rapid membrane protrusions, but these did not result in directional migration out of the tailbud (Fig. 7J-L, Movies 6 and 7). These results are consistent with our quantitative cell tracking and EMT marker analysis, and imply that Wnt signaling initiates the EMT whereas FGF signaling promotes completion and exit into the mesenchymal PM.

DISCUSSION

Wnt and FGF interactions ensure a steady movement of cells from the NMPs to the PM

Our results show that during mesoderm induction within the tailbud NMP population, Wnt signaling initiates the EMT event required for mesoderm induction and that FGF signaling subsequently promotes completion of the EMT (Fig. 7M). Upon Wnt inhibition, fewer cells enter the EMT transitional state from the NMPs, whereas loss of FGF signaling prevents cells from exiting EMT, causing them to remain trapped in the *vimr1/vimr2*-positive transitional state (Fig. 7M). Our results help explain previous observations that loss of Wnt signaling in the tailbud primarily causes an opposite response to the loss of FGF signaling with regard to the transcription of co-regulated genes (Stulberg et al., 2012). Since one signal promotes the transitional state and the other inhibits it, it follows that they should oppositely regulate specific target genes. In particular, many of the oppositely regulated genes are involved in cell adhesion, suggesting that Wnt signaling antagonizes cell-cell adhesion whereas FGF signaling promotes it. Interestingly, the same study also showed that Wnt and FGF positively regulate the signaling of one another (Stulberg et al., 2012). Based on our results, this positive interaction ensures that a continuous flow of cells enters and then exits the transitional EMT state during the generation of PM from NMPs.

The factors that function downstream of Wnt signaling to initiate EMT in NMPs remain unknown. Canonical EMT pathways, such as Snail repression of *cdh1*, do not appear to be relevant in this context, as embryos with loss of *snail1a* function (the *snail1* ortholog that is expressed in tailbud mesoderm) do not have deficits in mesoderm formation (Fior et al., 2012). Additionally, *cdh1* expression is uniform throughout the tailbud, without any clear difference between NMPs and mesodermal progenitors (Thisse and Thisse, 2005). Given that Wnt signaling promotes metastasis in a variety of cancers, the tailbud will serve as an important *in vivo* model to decipher the molecular mechanism of Wnt-induced EMT.

The role of FGF signaling during mesoderm induction changes between gastrula and post-gastrula stages

Our understanding of the molecular mechanisms of mesoderm induction is based largely on data from gastrula stages of development. The discovery that mesoderm continues to be induced after gastrulation from an NMP population in the tailbud raised the question of whether there are multiple ways to induce mesoderm or, alternatively, that the mechanism is entirely conserved during gastrula and tailbud stages of development. Here we show that the role of FGF signaling changes between the two periods of mesoderm induction. As opposed to gastrulation, where FGF

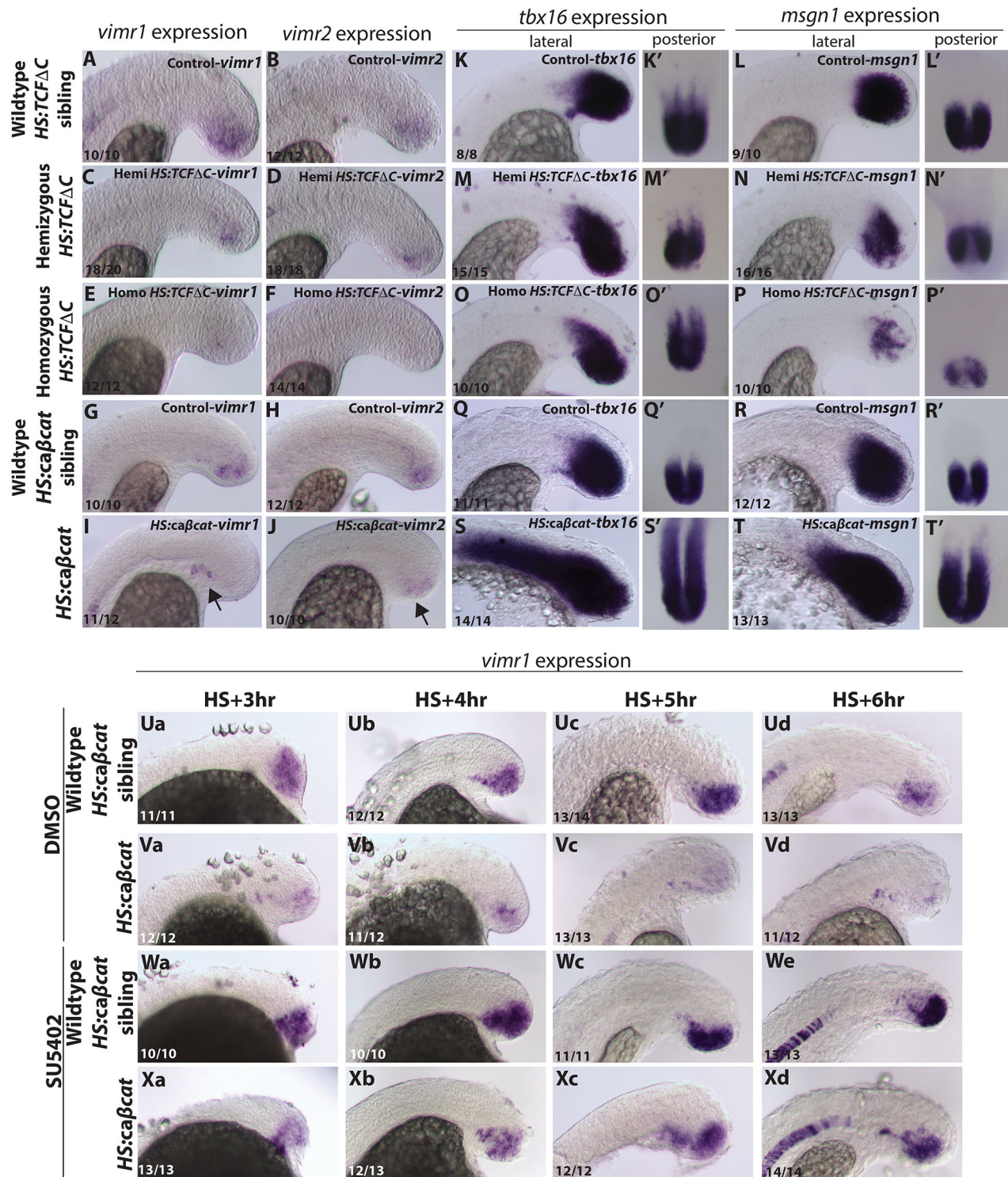


Fig. 6. Wnt promotes EMT initiation and cooperates with FGF to promote EMT termination in tailbud NMPs. (A-F) *vimr1* and *vimr2* expression was analyzed in 20-somite stage wild-type sibling (A,B), hemizygous *HS:TCFΔC* (C,D) and homozygous *HS:TCFΔC* (E,F) embryos. Wnt inhibition leads to the loss of *vimr1* and *vimr2*. (G-J) Expression of *vimr1* and *vimr2* was also analyzed in *HS:caβ-catenin* embryos (I,J) and their wild-type siblings (G,H). Wnt overactivation leads to a loss of *vimr1* and *vimr2* expression and a shift towards the ventral anterior portion of the tailbud (black arrow in I,J). (K-T') *tbx16* and *msgn1* expression was examined in control (K-L', Q-R'), hemizygous *HS:TCFΔC* (M-N'), homozygous *HS:TCFΔC* (O-P') and *HS:caβ-catenin* (S-T') embryos. Wnt inhibition had little effect on *tbx16* expression but led to decreased expression of *msgn1*. Wnt overactivation led to expansion of the *tbx16* and *msgn1* expression domains. (Ua-Xd) Epistasis experiments were performed to examine the control of *vimr1* expression by the Wnt and FGF signaling pathways. *HS:caβ-catenin* embryos were heat shocked at the 12-somite stage and treated with SU5402 or vehicle only (DMSO). These embryos were subsequently fixed 3 h, 4 h, 5 h and 6 h after heat shock induction for *in situ* hybridization. DMSO-treated control embryos exhibited consistent expression of *vimr1* during somitogenesis (Ua-d), whereas DMSO-treated *HS:caβ-catenin* embryos had decreased expression of the EMT marker in the tailbud (Va-d). Consistent with previous data (Fig. 3), FGF inhibitor-treated embryos had increased expression of *vimr1* (Wa-d). *HS:caβ-catenin* embryos in the presence of SU5402 maintained strong expression of *vimr1* (Xa-d). All tailbud images are lateral views, except where indicated otherwise.

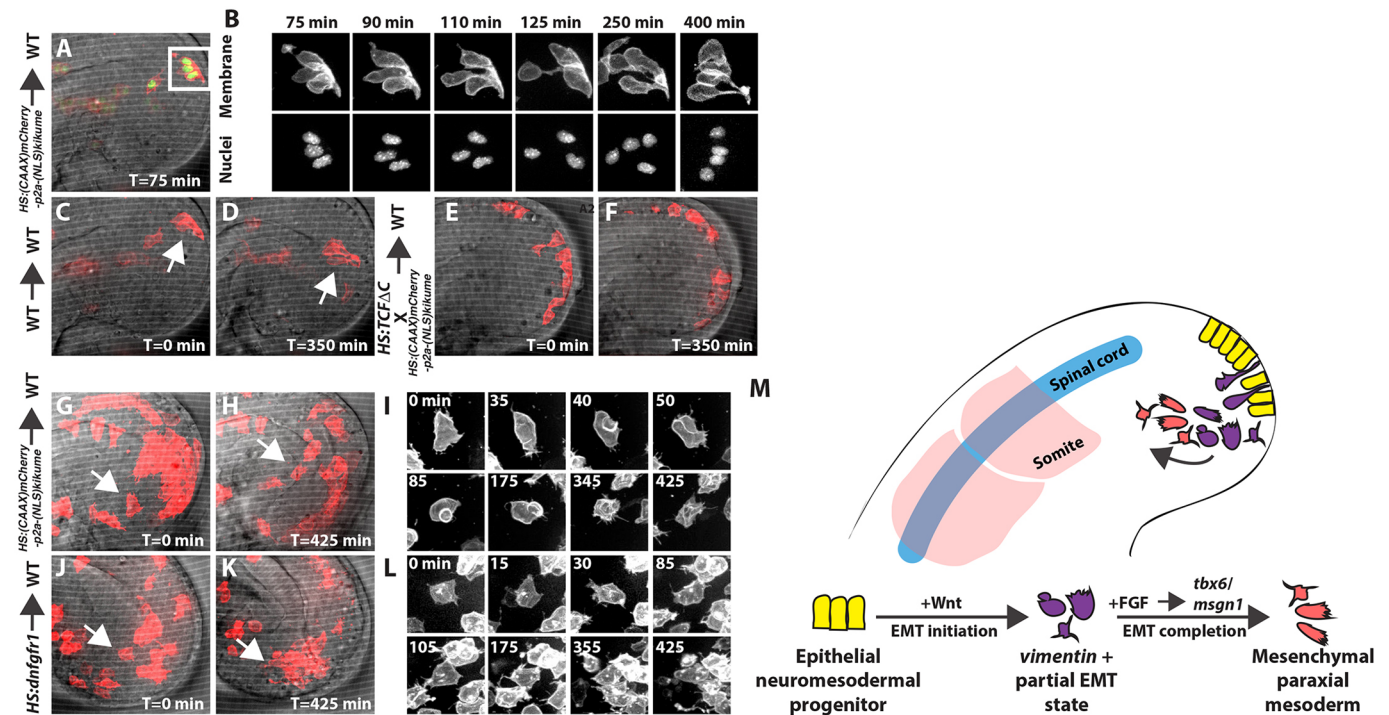


Fig. 7. Live imaging of tailbud EMT. (A-F) Transplanted *HS:(CAAX)mCherry-p2a-(NLS)kikume* cells were targeted to the NMP epithelium (A); the boxed region is shown in B. Time-lapse analysis shows that NMP epithelial cells undergo apical constriction and transition out of the epithelium but remain tethered to the epithelial layer by a stretched apical membrane ($t=125$ min; see also Movies 1 and 2; total of seven movies analyzed). The same embryo from A and B is shown in C and D at $t=0$ min (C) and $t=350$ min (D). Arrows (C,D) indicate cells that undergo the first EMT step over the course of the movie. Transplanted *HS:TCFAC* cells heat shocked at the bud stage fail to leave the NMP epithelium (compare F with E; see Movie 3; total of four movies analyzed). (G-L) Cells that have left the NMP epithelium eventually migrate out of the tailbud into the PM territory (G,H, arrow), and produce extensive membrane protrusions during this process (I; see Movies 4 and 5). Cells lacking FGF signaling fail to directionally migrate out of the tailbud (J,K, arrow), but still exhibit extensive membrane protrusions (L; the cell in the center of panels is the same as that indicated by an arrow in J,K; see Movies 6 and 7; total of four movies analyzed). (M) Model for two-step EMT. In the zebrafish tailbud, Wnt initiates EMT in the *sox2/ntla*-positive NMP population through regulation of unknown target(s). This leads to movement into a transitional zone, where they express the EMT markers *vimr1* and *vimr2*. Subsequently, FGF is required to terminate EMT and turn off early progenitor markers *ntla/sox2* by promoting *mshg1* and *tbx16* expression. This results in exit from the tailbud and maturation of these cells to form the PM.

signaling promotes mesoderm induction through the positive regulation of Brachyury expression, FGF signaling serves to repress Brachyury in NMPs (Amaya et al., 1993; Ciruna and Rossant, 2001; Delaune et al., 2005; Fletcher and Harland, 2008; Griffin et al., 1995; Isaacs et al., 1994; Schulte-Merker and Smith, 1995). In NMPs, FGF induces PM through positive regulation of *tbx16* and *mshg1* transcription, which in turn repress the NMP markers *sox2* and *ntla* and permit the completion of the mesodermal EMT event, allowing exit into the PM (Fig. 7M). In the chick, temporal loss of FGF signaling causes a loss of brachyury expression in the tailbud (Olivera-Martinez et al., 2012) 24 h after signal inhibition. Our experiments showed expanded *ntla* expression in the tailbud analyzed in embryos just 3 h after FGF inhibition. The result from chick embryos might reflect additional roles of FGF in the tailbud, such as the long-term maintenance of NMPs.

The variable usage of the FGF signaling pathway during gastrula and post-gastrula zebrafish mesoderm induction shows that there is considerable plasticity in the control of mesoderm induction within this species. Such variability might provide insight into the differential usage of the FGF pathway during gastrula stage mesoderm induction in the deuterostome lineage. For instance, within the deuterostomes, the echinoderm clade does not require FGF signaling for mesoderm induction during gastrulation (McCoon et al., 1996, 1998; Rottinger et al., 2008), yet all other major clades do, including vertebrates, tunicates, cephalochordates and hemichordates (Bertrand et al., 2011; Darras and Nishida, 2001;

Dorey and Amaya, 2010; Green et al., 2013; Imai et al., 2002; Kim and Nishida, 2001; Kimelman, 2006; Miya and Nishida, 2003; Yasuo and Hudson, 2007). This suggests that FGF signaling was required for mesoderm induction in the deuterostome ancestor, but this requirement was subsequently lost in the echinoderm lineage. Further analysis of the molecular mechanisms of mesoderm induction between gastrula and post-gastrula stages within and between species will better inform our understanding of the evolution and utilization of mesoderm-inducing gene networks.

Molecular control of a two-step EMT

EMT can be defined by several morphological and molecular measures, such as changes in cell shape and migratory activity, as well as the downregulation of epithelial-specific genes and upregulation of mesenchyme-specific genes. In the zebrafish tailbud, EMT has been defined primarily by changes in cell movement and morphology (Lawton et al., 2013; Manning and Kimelman, 2015). EMT and EMT-like events during development, homeostasis and metastasis are characterized by expression of the intermediate filament protein vimentin (Lowery et al., 2015). As such, vimentin is one of the most commonly used markers of cells undergoing EMT. We identified two *vimentin* genes in the zebrafish genome (*vimr1* and *vimr2*) and found that they are both expressed in the tailbud in precisely those cells that are actively undergoing EMT, between the initiation (Wnt-mediated) and termination (FGF-mediated) phases of the process. Although vimentin expression is

associated generally with the mesenchymal state, other work has demonstrated specific and strong expression of vimentin in a partial EMT state during chick epiboly (Futterman et al., 2011). Additionally, recent work indicates that a partial or intermediate EMT state is associated with more invasive and pathogenic cancer cells (Jolly et al., 2015; Nieto et al., 2016). Therefore, the vimentin expression often observed in actively metastasizing cells may reflect a partial EMT cellular condition.

EMT has traditionally been thought of as a binary single-step event, in which polarized epithelial cells transition directly to an invasive and migratory mesenchyme. Zebrafish PM formation, however, is a multistep process that includes an intermediate or partial EMT step (Manning and Kimelman, 2015; Row et al., 2011). Similarly, a growing body of experimental and theoretical evidence in several systems suggests that EMT involves multiple transitional states (Futterman et al., 2011; Grande et al., 2015; Lu et al., 2013; Mandal et al., 2016; Nieto et al., 2016; Revenu and Gilmour, 2009; Tian et al., 2013). Little is known about the molecular factors governing these intermediate states. During vertebrate mesoderm formation, both Wnt and FGF signaling promote the eventual formation of mesenchymal PM from the epithelial epiblast (Kiecker et al., 2016; Kimelman, 2006). Here we show that although both signals promote the formation of mesenchymal mesoderm from an epithelium, they have differential effects on the transitional or partial EMT state. Wnt signaling promotes the transitional state by initiating the EMT event, whereas FGF signaling inhibits the transitional state by regulating termination of the EMT.

Conclusions

The formation of the three primary germ layers was historically thought to occur exclusively during gastrulation. The discovery that mesoderm and ectoderm continue to be generated from a basal progenitor cell pool in the tailbud after gastrulation raises questions about the relatedness of mesoderm induction during and after gastrulation. We find that FGF has a unique role in mesoderm induction in the tailbud that is different from its role during gastrula stage mesoderm induction. This supports a model in which germ layer induction in the tailbud and the development of the posterior body is not a direct continuation of gastrulation, but rather a distinct embryonic process involving a specialized multi-germ layer competent progenitor (the NMP). Additionally, we further characterized the molecular control of a two-step EMT event during tailbud mesoderm induction that involves a distinct partial EMT phase. There is growing evidence that multistep EMT, with metastable partial EMT intermediates, is a common process, and that the partial EMT state is particularly pathogenic in disease conditions (Nieto et al., 2016). The zebrafish tailbud provides an excellent model to further characterize the molecular control and cell biological properties of multistep EMTs, for which there are currently few developmental models.

MATERIALS AND METHODS

In situ hybridization and immunohistochemistry

Single-probe whole-mount *in situ* hybridization was performed as previously described (Griffin et al., 1995). For immunohistochemistry, Tbx16 expression was detected in fixed embryos using a *Xenopus laevis* VegT antibody (ZIRC) at 1:1000, followed by Alexa Fluor 488-conjugated anti-mouse secondary (Thermo Fisher Scientific, A-11001, 1:500). Double-fluorescence *in situ* hybridization was performed as previously described (Martin and Kimelman, 2012).

Phylogenetic analysis of vimentin-related genes

Amino acid alignments were made using MUSCLE 3.7 on the CIPRES portal (<http://www.phylo.org/>) and alignment errors were corrected

manually (Edgar, 2004). Bayesian phylogenetic analysis was performed using MrBayes 3.2.2 with mixed-model option on the CIPRES portal (Ronquist and Huelsenbeck, 2003). Four independent runs of 1×10^6 generations each were performed with a sampling frequency of every 100 generations. A 'consensus tree' was generated from MrBayes from the last 9000 trees of each run (total of 36,000).

Fish lines and heat shocks

All zebrafish methods were approved by the Stony Brook University Institutional Animal Care and Use Committee. *HS:dnfgr1-GFP* (Lee et al., 2005), *HS:ca β -catenin* (Veldman et al., 2013), *HS:cafgr1* (Marques et al., 2008), *HS:mgn1-p2a-NLS-kikume* (Row et al., 2016), *HS:TCFAC-GFP* (Martin and Kimelman, 2012), *HS:tbx16-p2a-NLS-kikume* (this study) and *HS:CAAXmCherry-p2a-NLS-kikume* (this study) fish provided embryos that were heat shocked at the previously described temperatures for 30 min. Transgenic embryos were sorted from their wild-type siblings based on fluorescence or unique phenotypes. Heterozygous *spt^{h104}* mutant fish were used for *tbx16* loss-of-function experiments (Ho and Kane, 1990).

Cell transplantation

Cell transplantation was performed as previously described with the following adjustments (Martin and Kimelman, 2010). Donor embryos were injected with 2% Rhodamine or Fluorescein-dextran at the one-cell stage. Cells from sphere stage donor embryos were transplanted into the ventral margin of unlabeled shield stage hosts using a CellTram vario (Eppendorf).

For lineage tracing, a mix of 2% Fluorescein-dextran and 25 pg Tol2 plasmid encoding NLS-kikume with or without the *tbx16* or *mgn1* gene was injected into wild-type or *HS:dnfgr1* donors. Transplants were conducted as above with heat shocks at bud stage and analysis at 30 hpf.

Kikume photoconversion, microscopy and image analysis

Tailbuds of *NLS-kikume* mRNA-injected (25 pg per embryo) embryos were photoconverted in the NMP region and imaged using a Leica DMI6000B inverted microscope at 20 \times magnification or using a spinning disc confocal microscope (CSU-10, Yokogawa; AxioImager, Carl Zeiss) equipped with a camera (EM-CCD; Hamamatsu Photonics) with a 20 \times differential contrast objective. Stacks of tailbud images, spaced 5 μ m apart, were taken every 5 min for 5 h beginning at the 12-somite stage. For lineage analysis, transplants were imaged at 30 hpf using both the inverted microscope with a 40 \times objective and the spinning disc confocal microscope with a 10 \times objective. Live imaging of *HS:CAAXmCherry-p2a-NLS-kikume* transgenic cells was performed by spinning disc confocal microscopy using a 40 \times dipping objective lens at 5 min intervals for 8 h.

Time-lapse movies were analyzed on ImageJ and Imaris (Bitplane). The tracking of photoconverted nuclei was performed on Imaris through the spot detection scene. The generated tracks were corrected manually, and the mean track speed and displacement were calculated using Imaris.

Drug treatment

For the time-lapse experiments, *NLS-kikume* mRNA-injected embryos were heat shocked at the 10-somite stage, dechorionated immediately, then 30 min after the heat shock the embryos were placed in either 50 μ M SU5402 (Sigma) or an equivalent volume of DMSO for 2.5 h. Subsequently, the embryos were mounted in low melting point agarose containing 50 μ M drug or vehicle for microscopy imaging.

Acknowledgements

We thank Neal Bhattacharji for excellent fish care.

Competing interests

The authors declare no competing or financial interests.

Author contributions

D.Q.M. analyzed the data and edited the manuscript. S.C.K. and R.H.R. performed experiments and edited the manuscript. H.G. and B.L.M. performed experiments, analyzed the data and wrote the manuscript.

Funding

This work was supported by a National Institutes of Health training grant [T32 GM008468] to H.G., a Stony Brook University EURECA fellowship to S.C.K., a National Cancer Institute [4R00CA154870-03] grant to D.Q.M., and American Heart Association [13SDG14360032] and National Science Foundation [IOS1452928] grants to B.L.M. D.Q.M. and B.L.M. also acknowledge support from Stony Brook University startup funds. Deposited in PMC for release after 12 months.

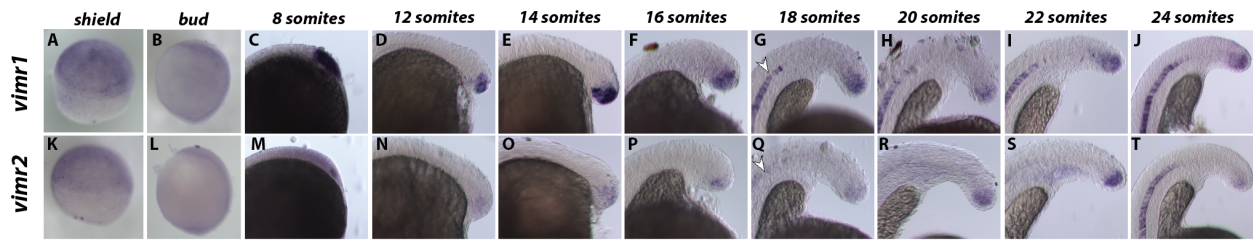
Supplementary information

Supplementary information available online at <http://dev.biologists.org/lookup/doi/10.1242/dev.143578.supplemental>

References

- Acloque, H., Adams, M. S., Fishwick, K., Bronner-Fraser, M. and Nieto, M. A.** (2009). Epithelial-mesenchymal transitions: the importance of changing cell state in development and disease. *J. Clin. Invest.* **119**, 1438-1449.
- Akai, J., Halley, P. A. and Storey, K. G.** (2005). FGF-dependent Notch signaling maintains the spinal cord stem zone. *Genes Dev.* **19**, 2877-2887.
- Amaya, E., Musci, T. J. and Kirschner, M. W.** (1991). Expression of a dominant negative mutant of the FGF receptor disrupts mesoderm formation in *Xenopus* embryos. *Cell* **66**, 257-270.
- Amaya, E., Stein, P. A., Musci, T. J. and Kirschner, M. W.** (1993). FGF signalling in the early specification of mesoderm in *Xenopus*. *Development* **118**, 477-487.
- Beck, C. W.** (2015). Development of the vertebrate tailbud. *Wiley Interdiscip. Rev. Dev. Biol.* **4**, 33-44.
- Bertrand, S., Camasses, A., Somorjai, I., Belgacem, M. R., Chabrol, O., Escande, M.-L., Pontarotti, P. and Escriva, H.** (2011). Amphioxus FGF signaling predicts the acquisition of vertebrate morphological traits. *Proc. Natl. Acad. Sci. USA* **108**, 9160-9165.
- Bouldin, C. M., Manning, A. J., Peng, Y.-H., Farr, G. H., 3rd, Hung, K. L., Dong, A. and Kimelman, D.** (2015). Wnt signaling and *tbx16* form a bistable switch to commit bipotential progenitors to mesoderm. *Development* **142**, 2499-2507.
- Cerdà, J., Conrad, M., Markl, J., Brand, M. and Herrmann, H.** (1998). Zebrafish vimentin: molecular characterization, assembly properties and developmental expression. *Eur. J. Cell Biol.* **77**, 175-187.
- Ciruna, B. and Rossant, J.** (2001). FGF signaling regulates mesoderm cell fate specification and morphogenetic movement at the primitive streak. *Dev. Cell* **1**, 37-49.
- Darras, S. and Nishida, H.** (2001). The BMP signaling pathway is required together with the FGF pathway for notochord induction in the ascidian embryo. *Development* **128**, 2629-2638.
- Delaune, E., Lemaire, P. and Kodjabachian, L.** (2005). Neural induction in *Xenopus* requires early FGF signalling in addition to BMP inhibition. *Development* **132**, 299-310.
- Deng, C. X., Wynshaw-Boris, A., Shen, M. M., Daugherty, C., Ornitz, D. M. and Leder, P.** (1994). Murine FGFR-1 is required for early postimplantation growth and axial organization. *Genes Dev.* **8**, 3045-3057.
- Dorey, K. and Amaya, E.** (2010). FGF signalling: diverse roles during early vertebrate embryogenesis. *Development* **137**, 3731-3742.
- Dubrulle, J., McGrew, M. J. and Pourquie, O.** (2001). FGF signaling controls somite boundary position and regulates segmentation clock control of spatiotemporal Hox gene activation. *Cell* **106**, 219-232.
- Edgar, R. C.** (2004). MUSCLE: multiple sequence alignment with high accuracy and high throughput. *Nucleic Acids Res.* **32**, 1792-1797.
- Fior, R., Maxwell, A. A., Ma, T. P., Vezzano, A., Moens, C. B., Amacher, S. L., Lewis, J. and Saude, L.** (2012). The differentiation and movement of presomitic mesoderm progenitor cells are controlled by Mesogenin 1. *Development* **139**, 4656-4665.
- Fletcher, R. B. and Harland, R. M.** (2008). The role of FGF signaling in the establishment and maintenance of mesodermal gene expression in *Xenopus*. *Dev. Dyn.* **237**, 1243-1254.
- Futterman, M. A., García, A. J. and Zamir, E. A.** (2011). Evidence for partial epithelial-to-mesenchymal transition (pEMT) and recruitment of motile blastoderm edge cells during avian epiboly. *Dev. Dyn.* **240**, 1502-1511.
- Garriock, R. J., Chalamasetty, R. B., Kennedy, M. W., Canizales, L. C., Lewandoski, M. and Yamaguchi, T. P.** (2015). Lineage tracing of neuromesodermal progenitors reveals novel Wnt-dependent roles in trunk progenitor cell maintenance and differentiation. *Development* **142**, 1628-1638.
- Gouti, M., Tsakiridis, A., Wymeersch, F. J., Huang, Y., Kleinjung, J., Wilson, V. and Briscoe, J.** (2014). In vitro generation of neuromesodermal progenitors reveals distinct roles for wnt signalling in the specification of spinal cord and paraxial mesoderm identity. *PLoS Biol.* **12**, e1001937.
- Grande, M. T., Sánchez-Laorden, B., López-Blau, C., De Frutos, C. A., Boutet, A., Arévalo, M., Rowe, R. G., Weiss, S. J., López-Novoa, J. M. and Nieto, M. A.** (2015). Snail1-induced partial epithelial-to-mesenchymal transition drives renal fibrosis in mice and can be targeted to reverse established disease. *Nat. Med.* **21**, 989-997.
- Green, S. A., Norris, R. P., Terasaki, M. and Lowe, C. J.** (2013). FGF signaling induces mesoderm in the hemichordate *Saccoglossus kowalevskii*. *Development* **140**, 1024-1033.
- Griffin, K., Patient, R. and Holder, N.** (1995). Analysis of FGF function in normal and no tail zebrafish embryos reveals separate mechanisms for formation of the trunk and the tail. *Development* **121**, 2983-2994.
- Griffin, K. J., Amacher, S. L., Kimmel, C. B. and Kimelman, D.** (1998). Molecular identification of spadetail: regulation of zebrafish trunk and tail mesoderm formation by T-box genes. *Development* **125**, 3379-3388.
- Henrique, D., Abranches, E., Verrier, L. and Storey, K. G.** (2015). Neuromesodermal progenitors and the making of the spinal cord. *Development* **142**, 2864-2875.
- Herrmann, H., Hofmann, I. and Franke, W. W.** (1992). Identification of a nonapeptide motif in the vimentin head domain involved in intermediate filament assembly. *J. Mol. Biol.* **223**, 637-650.
- Ho, R. K. and Kane, D. A.** (1990). Cell-autonomous action of zebrafish *spt-1* mutation in specific mesodermal precursors. *Nature* **348**, 728-730.
- Hubaud, A. and Pourquie, O.** (2014). Signalling dynamics in vertebrate segmentation. *Nat. Rev. Mol. Cell Biol.* **15**, 709-721.
- Imai, K. S., Satoh, N. and Satou, Y.** (2002). Early embryonic expression of FGF4/6/9 gene and its role in the induction of mesenchyme and notochord in *Ciona savignyi* embryos. *Development* **129**, 1729-1738.
- Isaacs, H. V., Pownall, M. E. and Slack, J. M.** (1994). eFGF regulates Xbra expression during *Xenopus* gastrulation. *EMBO J.* **13**, 4469-4481.
- Jolly, M. K., Boareto, M., Huang, B., Jia, D., Lu, M., Ben-Jacob, E., Onuchic, J. N. and Levine, H.** (2015). Implications of the hybrid epithelial/mesenchymal phenotype in metastasis. *Front. Oncol.* **5**, 155.
- Jurberg, A. D., Aires, R., Nóvoa, A., Rowland, J. E. and Mallo, M.** (2014). Compartment-dependent activities of Wnt3a/beta-catenin signaling during vertebrate axial extension. *Dev. Biol.* **394**, 253-263.
- Kiecker, C., Bates, T. and Bell, E.** (2016). Molecular specification of germ layers in vertebrate embryos. *Cell. Mol. Life Sci.* **73**, 923-947.
- Kim, G. J. and Nishida, H.** (2001). Role of the FGF and MEK signaling pathway in the ascidian embryo. *Dev. Growth Differ.* **43**, 521-533.
- Kimelman, D.** (2006). Mesoderm induction: from caps to chips. *Nat. Rev. Genet.* **7**, 360-372.
- Kimelman, D.** (2016). Tales of tails (and trunks): forming the posterior body in vertebrate embryos. *Curr. Top. Dev. Biol.* **116**, 517-536.
- Kimelman, D. and Kirschner, M.** (1987). Synergistic induction of mesoderm by FGF and TGF-beta and the identification of an mRNA coding for FGF in the early *Xenopus* embryo. *Cell* **51**, 869-877.
- Kimelman, D. and Martin, B. L.** (2012). Anterior-posterior patterning in early development: three strategies. *Wiley Interdiscip. Rev. Dev. Biol.* **1**, 253-266.
- Kimelman, D., Abraham, J. A., Haaparanta, T., Palisi, T. M. and Kirschner, M. W.** (1988). The presence of fibroblast growth factor in the frog egg: its role as a natural mesoderm inducer. *Science* **242**, 1053-1056.
- Kondoh, H. and Takemoto, T.** (2012). Axial stem cells deriving both posterior neural and mesodermal tissues during gastrulation. *Curr. Opin. Genet. Dev.* **22**, 374-380.
- Latinkic, B. V., Umbhauer, M., Neal, K. A., Lerchner, W., Smith, J. C. and Cunliffe, V.** (1997). The *Xenopus* Brachyury promoter is activated by FGF and low concentrations of activin and suppressed by high concentrations of activin and by paired-type homeodomain proteins. *Genes Dev.* **11**, 3265-3276.
- Lawton, A. K., Nandi, A., Stulberg, M. J., Dray, N., Sneddon, M. W., Pontius, W., Emonet, T. and Holley, S. A.** (2013). Regulated tissue fluidity steers zebrafish body elongation. *Development* **140**, 573-582.
- Lee, Y., Grill, S., Sanchez, A., Murphy-Ryan, M. and Poss, K. D.** (2005). Fgf signaling instructs position-dependent growth rate during zebrafish fin regeneration. *Development* **132**, 5173-5183.
- Lowery, J., Kuczmarzski, E. R., Herrmann, H. and Goldman, R. D.** (2015). Intermediate filaments play a pivotal role in regulating cell architecture and function. *J. Biol. Chem.* **290**, 17145-17153.
- Lu, M., Jolly, M. K., Levine, H., Onuchic, J. N. and Ben-Jacob, E.** (2013). MicroRNA-based regulation of epithelial-hybrid-mesenchymal fate determination. *Proc. Natl. Acad. Sci. USA* **110**, 18144-18149.
- Mandal, M., Ghosh, B., Anura, A., Mitra, P., Pathak, T. and Chatterjee, J.** (2016). Modeling continuum of epithelial mesenchymal transition plasticity. *Integr. Biol.* **8**, 167-176.
- Manning, A. J. and Kimelman, D.** (2015). *Tbx16* and *Msgn1* are required to establish directional cell migration of zebrafish mesodermal progenitors. *Dev. Biol.* **406**, 172-185.
- Marques, S. R., Lee, Y., Poss, K. D. and Yelon, D.** (2008). Reiterative roles for FGF signaling in the establishment of size and proportion of the zebrafish heart. *Dev. Biol.* **321**, 397-406.
- Martin, B. L.** (2016). Factors that coordinate mesoderm specification from neuromesodermal progenitors with segmentation during vertebrate axial extension. *Semin. Cell Dev. Biol.* **49**, 59-67.
- Martin, B. L. and Kimelman, D.** (2008). Regulation of canonical Wnt signaling by Brachyury is essential for posterior mesoderm formation. *Dev. Cell* **15**, 121-133.

- Martin, B. L. and Kimelman, D.** (2009). Wnt signaling and the evolution of embryonic posterior development. *Curr. Biol.* **19**, R215-R219.
- Martin, B. L. and Kimelman, D.** (2010). Brachyury establishes the embryonic mesodermal progenitor niche. *Genes Dev.* **24**, 2778-2783.
- Martin, B. L. and Kimelman, D.** (2012). Canonical Wnt signaling dynamically controls multiple stem cell fate decisions during vertebrate body formation. *Dev. Cell* **22**, 223-232.
- Mathis, L., Kulesa, P. M. and Fraser, S. E.** (2001). FGF receptor signalling is required to maintain neural progenitors during Hensen's node progression. *Nat. Cell Biol.* **3**, 559-566.
- McCoon, P. E., Angerer, R. C. and Angerer, L. M.** (1996). SpFGFR, a new member of the fibroblast growth factor receptor family, is developmentally regulated during early sea urchin development. *J. Biol. Chem.* **271**, 20119-20125.
- McCoon, P. E., Blackstone, E., Angerer, R. C. and Angerer, L. M.** (1998). Sea urchin FGFR muscle-specific expression: posttranscriptional regulation in embryos and adults. *Dev. Biol.* **200**, 171-181.
- Mitrani, E., Gruenbaum, Y., Shohat, H. and Ziv, T.** (1990). Fibroblast growth factor during mesoderm induction in the early chick embryo. *Development* **109**, 387-393.
- Miya, T. and Nishida, H.** (2003). An Ets transcription factor, HrEts, is target of FGF signaling and involved in induction of notochord, mesenchyme, and brain in ascidian embryos. *Dev. Biol.* **261**, 25-38.
- Nieto, M. A., Huang, R. Y.-J., Jackson, R. A. and Thiery, J. P.** (2016). Emt: 2016. *Cell* **166**, 21-45.
- Olivera-Martinez, I., Harada, H., Halley, P. A. and Storey, K. G.** (2012). Loss of FGF-dependent mesoderm identity and rise of endogenous retinoid signalling determine cessation of body axis elongation. *PLoS Biol.* **10**, e1001415.
- Ramkumar, N., Omelchenko, T., Silva-Gagliardi, N. F., McGlade, C. J., Wijnholds, J. and Anderson, K. V.** (2016). Crumbs2 promotes cell ingress ion during the epithelial-to-mesenchymal transition at gastrulation. *Nat. Cell Biol.* **18**, 1281-1291.
- Revenu, C. and Gilmour, D.** (2009). EMT 2.0: shaping epithelia through collective migration. *Curr. Opin. Genet. Dev.* **19**, 338-342.
- Ronquist, F. and Huelsenbeck, J. P.** (2003). MrBayes 3: Bayesian phylogenetic inference under mixed models. *Bioinformatics* **19**, 1572-1574.
- Rottinger, E., Saudemont, A., Duboc, V., Besnardeau, L., McClay, D. and Lepage, T.** (2008). FGF signals guide migration of mesenchymal cells, control skeletal morphogenesis and regulate gastrulation during sea urchin development. *Development* **135**, 353-365.
- Row, R. H., Maitre, J.-L., Martin, B. L., Stockinger, P., Heisenberg, C.-P. and Kimelman, D.** (2011). Completion of the epithelial to mesenchymal transition in zebrafish mesoderm requires Spadetail. *Dev. Biol.* **354**, 102-110.
- Row, R. H., Tsotras, S. R., Goto, H. and Martin, B. L.** (2016). The zebrafish tailbud contains two independent populations of midline progenitor cells that maintain long-term germ layer plasticity and differentiate in response to local signaling cues. *Development* **143**, 244-254.
- Schulte-Merker, S. and Smith, J. C.** (1995). Mesoderm formation in response to Brachyury requires FGF signalling. *Curr. Biol.* **5**, 62-67.
- Slack, J. M. W., Darlington, B. G., Heath, J. K. and Godsave, S. F.** (1987). Mesoderm induction in early *Xenopus* embryos by heparin-binding growth factors. *Nature* **326**, 197-200.
- Steventon, B., Duarte, F., Lagadec, R., Mazan, S., Nicolas, J.-F. and Hirsinger, E.** (2016). Species-specific contribution of volumetric growth and tissue convergence to posterior body elongation in vertebrates. *Development* **143**, 1732-1741.
- Stulberg, M. J., Lin, A., Zhao, H. and Holley, S. A.** (2012). Crosstalk between Fgf and Wnt signaling in the zebrafish tailbud. *Dev. Biol.* **369**, 298-307.
- Thisse, C. and Thisse, B.** (2005). High throughput expression analysis of ZF-models consortium clones. *ZFIN Direct Submission*, <http://zfin.org/ZDB-PUB-051025-1>.
- Tian, X.-J., Zhang, H. and Xing, J.** (2013). Coupled reversible and irreversible bistable switches underlying TGFbeta-induced epithelial to mesenchymal transition. *Biophys. J.* **105**, 1079-1089.
- Tsakiridis, A., Huang, Y., Blin, G., Skylaki, S., Wymeersch, F., Osorno, R., Economou, C., Karagianni, E., Zhao, S., Lowell, S. et al.** (2014). Distinct Wnt-driven primitive streak-like populations reflect in vivo lineage precursors. *Development* **141**, 1209-1221.
- Veldman, M. B., Zhao, C., Gomez, G. A., Lindgren, A. G., Huang, H., Yang, H., Yao, S., Martin, B. L., Kimelman, D. and Lin, S.** (2013). Transdifferentiation of fast skeletal muscle into functional endothelium in vivo by transcription factor Etv2. *PLoS Biol.* **11**, e1001590.
- Wymeersch, F. J., Huang, Y., Blin, G., Cambrey, N., Wilkie, R., Wong, F. C. K. and Wilson, V.** (2016). Position-dependent plasticity of distinct progenitor types in the primitive streak. *Elife* **5**, e10042.
- Yabe, T. and Takada, S.** (2012). Mesogenin causes embryonic mesoderm progenitors to differentiate during development of zebrafish tail somites. *Dev. Biol.* **370**, 213-222.
- Yamaguchi, T. P., Harpal, K., Henkemeyer, M. and Rossant, J.** (1994). fgfr-1 is required for embryonic growth and mesodermal patterning during mouse gastrulation. *Genes Dev.* **8**, 3032-3044.
- Yasuo, H. and Hudson, C.** (2007). FGF8/17/18 functions together with FGF9/16/20 during formation of the notochord in *Ciona* embryos. *Dev. Biol.* **302**, 92-103.
- Ye, X. and Weinberg, R. A.** (2015). Epithelial-mesenchymal plasticity: a central regulator of cancer progression. *Trends Cell Biol.* **25**, 675-686.



Goto et al. Supplemental Figure 1

Supplemental Figure 1. Time course expression of vimentin related genes

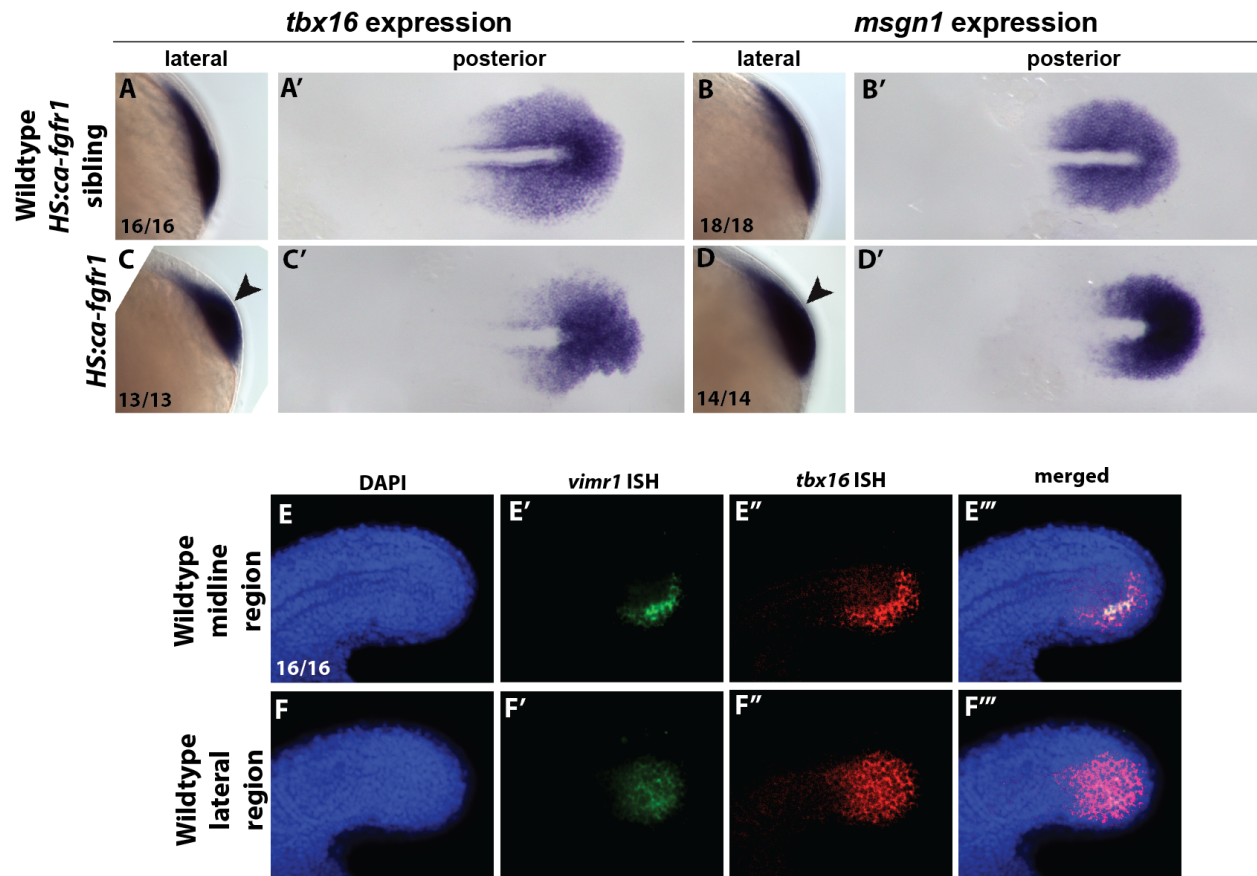
Vimr1 (A-J) and *Vimr2* (K-T) expression in wildtype embryos fixed at different stages. The beginning of notochord expression at the 18-somite stage is indicated by arrowheads (G and Q). Shield staged embryos were taken laterally with the shield towards the right. Embryos from 8-somite stage and onward were taken laterally with anterior towards the bottom.



Goto et al. Supplemental Figure 2

Supplemental Figure 2. Phylogenetic analysis of intermediate filaments

Bayesian phylogenetic analysis of zebrafish vimentin-like genes with other intermediate filaments with laminin genes serving as an outgroup. The numbers at the node specify Bayesian posterior probabilities. Species abbreviations with common names in parentheses: Ca, *Carassius auratus* (goldfish); Ce, *Caenorhabditis elegans* (nematode); Clf, *Canis lupus familiaris* (Dog); Dm, *Drosophila melanogaster* (fruit fly); Dr, *Danio rerio* (Zebrafish); Hs, *Homo sapiens* (human); Lf, *Lampetra fluviatilis* (Lamprey); Mm, *Mus musculus* (mouse); On, *Oreochromis niloticus* (Nile tilapia); Sp, *Stegastes partitus* (bicolor damselfish); Tr, *Takifugu rubripes* (pufferfish); Xt, *Xenopus tropicalis* (frog)



Goto et al. Supplemental Figure 3

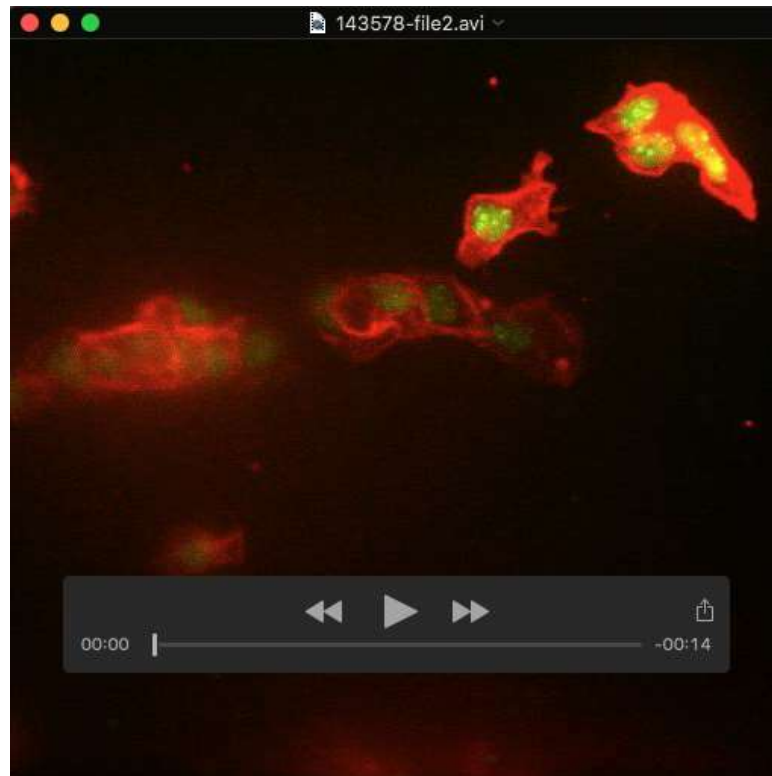
Supplemental Figure 3. Expression of mesodermal maturation genes in FGF overactivated tailbud and expression domains of *vimr1* and *tbx16* in the wildtype tailbud. *HS:cafgfr1* and wildtype embryos were heat-shocked at bud stage and fixed at 8-somite stage to examine the effect of FGF overactivation on maturation gene expression. Overactivation of FGF leads to strong expression of *tbx16* and *msgn1*, which expands into the NMP region (C, C', D, D') compared to the control (A, A', B, B'). Double fluorescent *in situ* hybridization of *tbx16* and *vimr1* in a wild-type 20-somite stage embryo. As the mesodermal progenitors move from the dorsal region to ventral region, the cells turn on *vimr1* and *tbx16* (E, E', E'', E'''). However, as the cells enter the maturation zone in the lateral regions, the cells turn off *vimr1* (F, F', F'', F''').

Table S1. Statistics for time lapse tracking. P values were calculated by Student's t-test. S indicates significant ($p < 0.05$), while NS implies nonsignificant ($p > 0.05$).

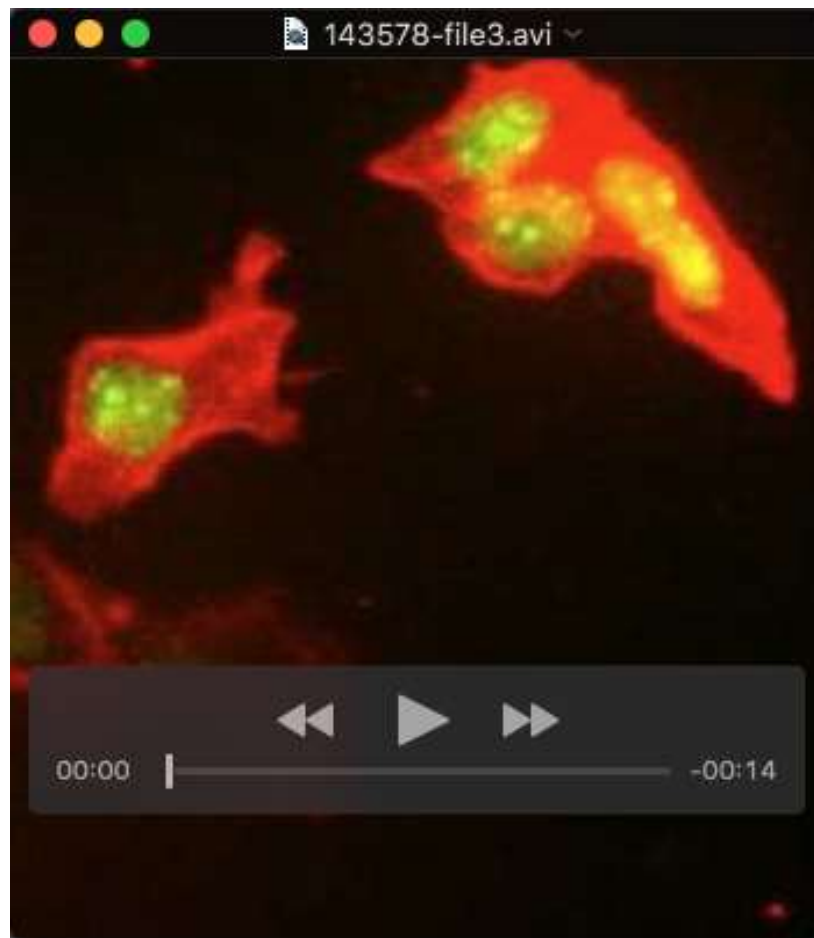
Embryo	number of embryos	Total tracks	Displacement		Mean Track Speed		Track straightness	
			P val compared to wildtype-DMSO	P val compared to HStbx16-SU5402	P val compared to wildtype-DMSO	P val compared to HStbx16-SU5402	P val compared to wildtype-DMSO	P val compared to HStbx16-SU5402
wildtype-DMSO	4	268						
HS:tbx16-DMSO	3	177	p=0.7425; NS	p=0.433; NS	p=0.0323; S	p=0.2539; NS	p=0.1601; NS	p=0.9717; NS
wildtype-SU5402	3	143	p=0.0323; S	p=0.0073; S	p=0.0073; S	p=0.0151; S	p=0.1886; NS	p=0.1116; NS
HS:tbx16-SU5402	3	223						
HS:caFGFr1-DMSO	3	169	p=0.5225; NS		p=0.0065; S		p=0.3332; NS	

Table S2. Raw data of transplanted lineage analysis and statistics. P values were calculated by Fisher's exact test. S indicates significant ($p < 0.05$), while NS denotes nonsignificant ($p > 0.05$).

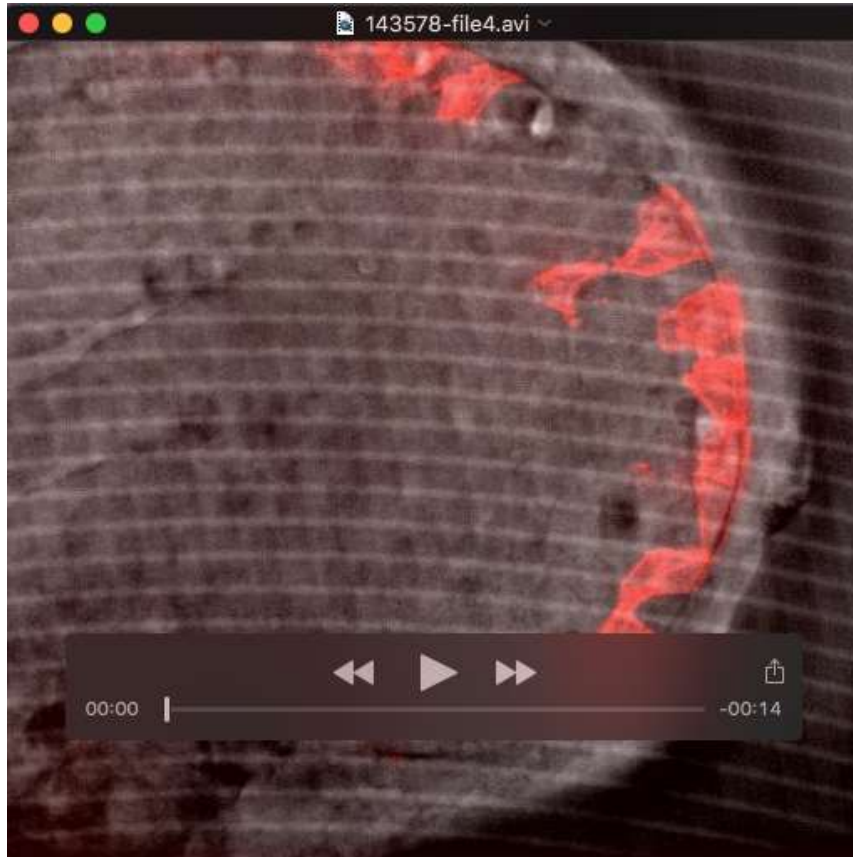
Embryo	number of embryos	Total muscle cells	Total nonmuscle cells	% muscle	% nonmuscle	P val compared to wildtype	P val compared to dnfgf
wildtype	10	167	68	71.064	28.936		
HS:dnfgfr1	10	33	127	20.625	79.375	$p < 0.0001$; S	
pmsgn1/wildtype	9	234	88	72.671	27.329	$p = 0.7028$; NS	
pmsgn1/HS:dnfgfr1	10	216	191	53.071	46.929	$p < 0.0001$; S	$p < 0.0001$; S
ptbx16/wildtype	8	177	96	64.835	35.165	$p = 0.153$; NS	
ptbx16/HS:dnfgfr1	9	97	81	54.494	45.506	$p = 0.0006$; S	$p < 0.0001$; S



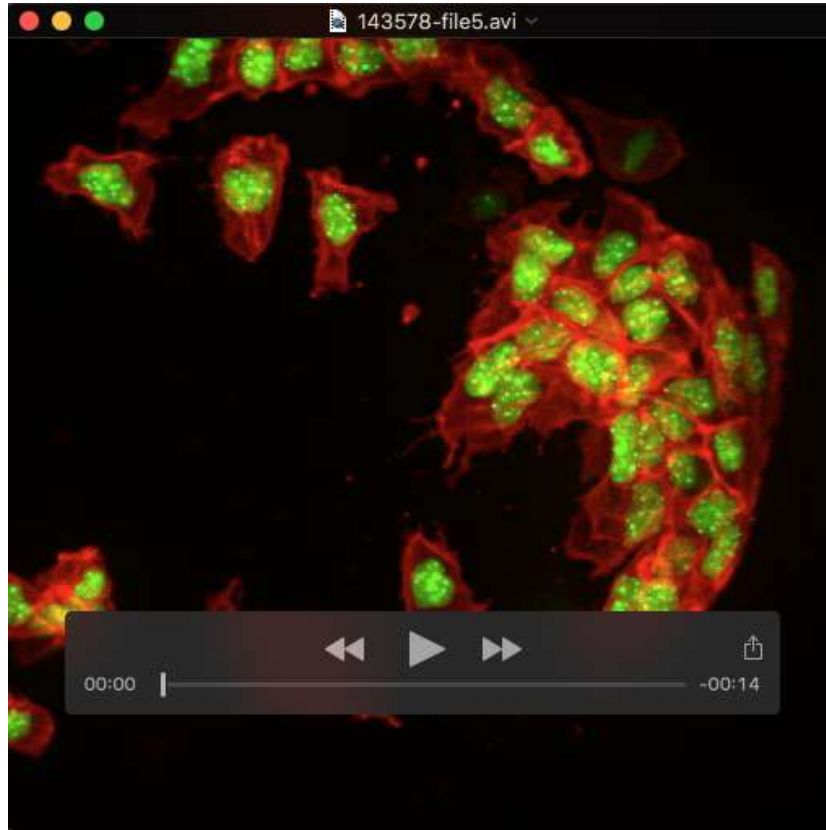
Movie 1. Time lapse movie of transplanted *HS:(CAAX)mCherry-p2a-(NLS)kikume* during the 1st EMT step. Cells of interest are in the upper right of the movie. Images were acquired every 5 minutes for 8 hours.



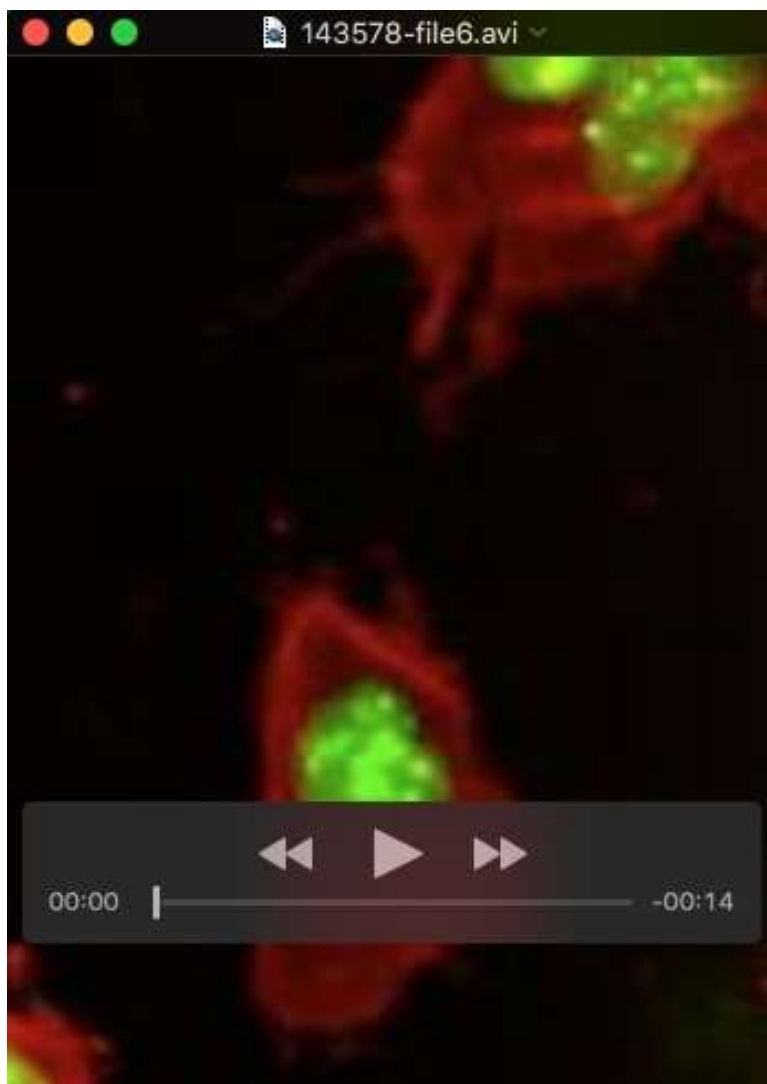
Movie 2. Cropped version of movie 1, focusing on cells of interest.



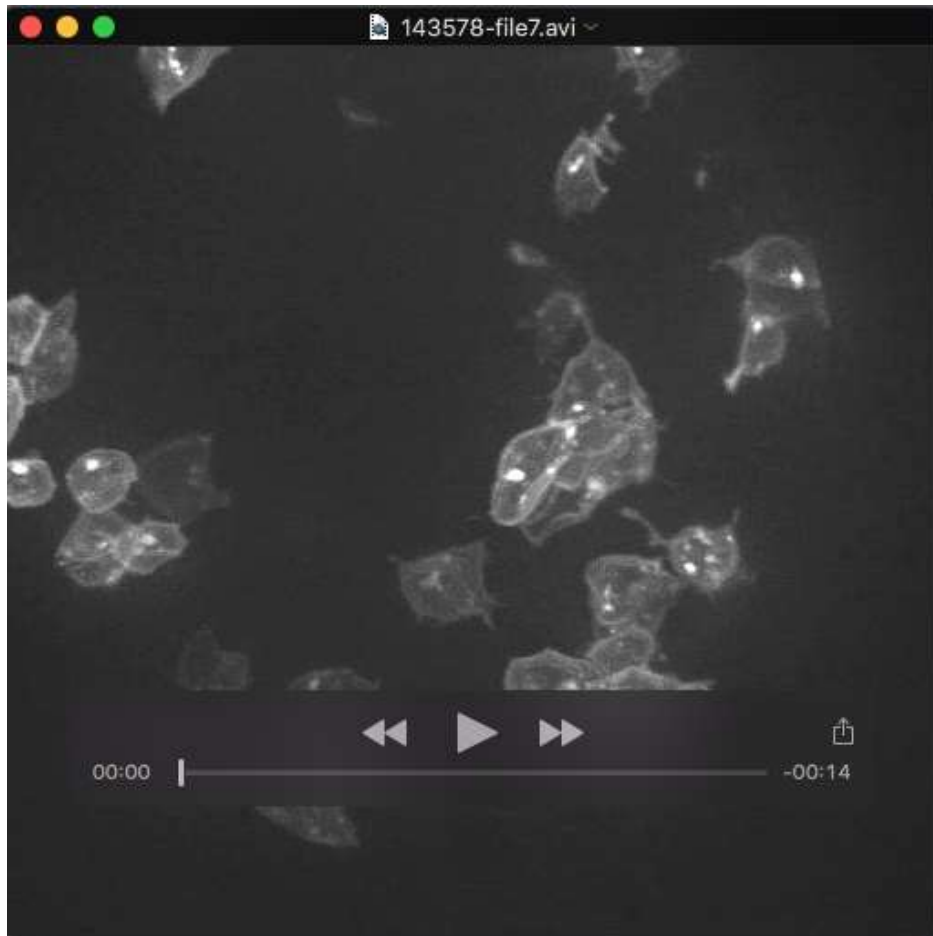
Movie 3. Time lapse movie of transplanted *HS:TCF Δ C* cells. . Images were acquired every 5 minutes for 8 hours.



Movie 4. Time lapse movie of transplanted *HS:(CAAX)mCherry-p2a-(NLS)kikume* during the 2nd EMT step. The cell of interest is in the lower left of the movie. . Images were acquired every 5 minutes for 8 hours.



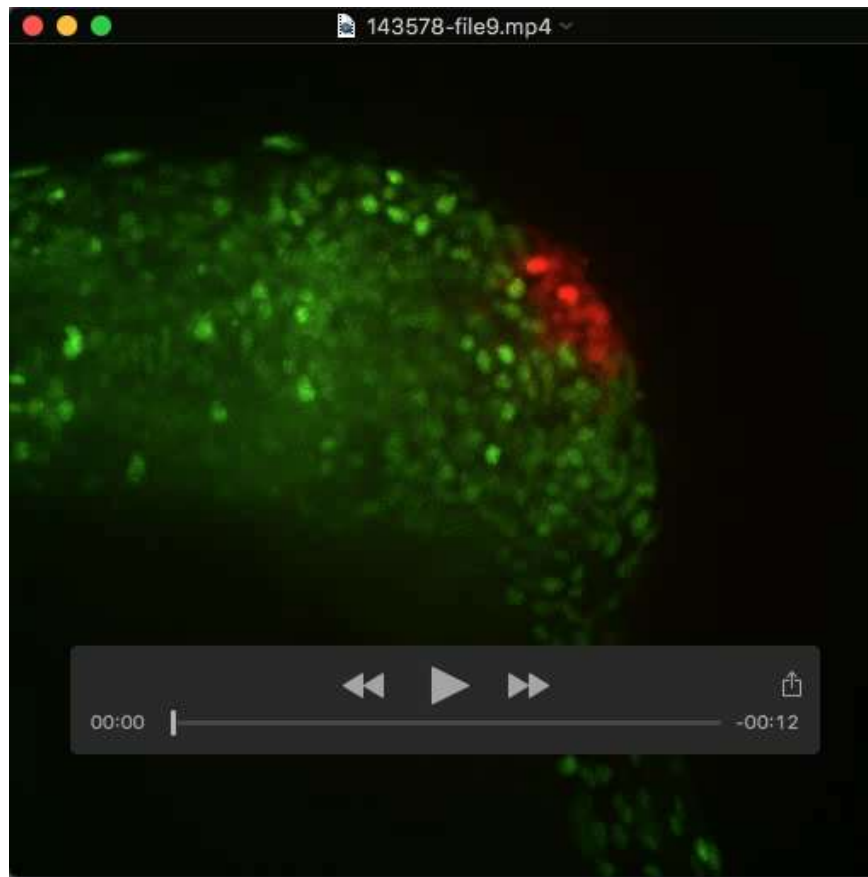
Movie 5. Cropped version of movie 4, focusing on the cell of interest.



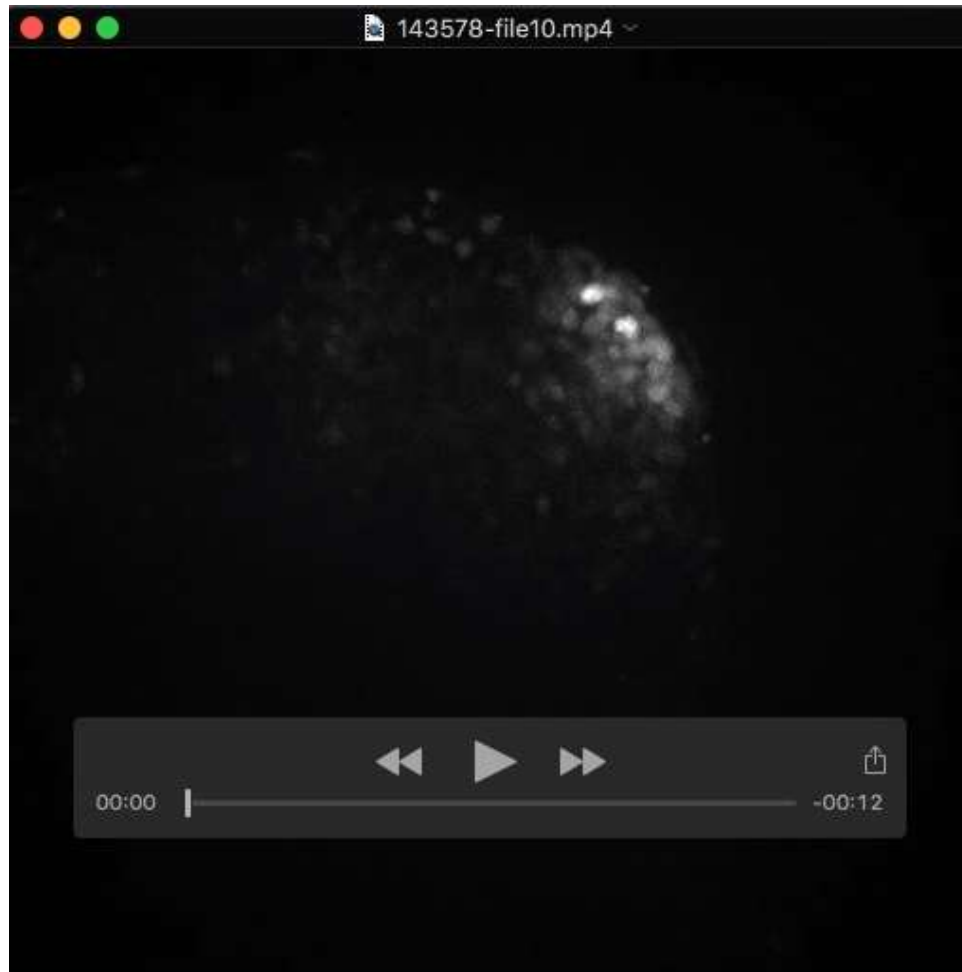
Movie 6. Time lapse movie of transplanted *HS:dnfgfr1* cells. The cell of interest is in the lower left of the movie. . Images were acquired every 5 minutes for 8 hours.



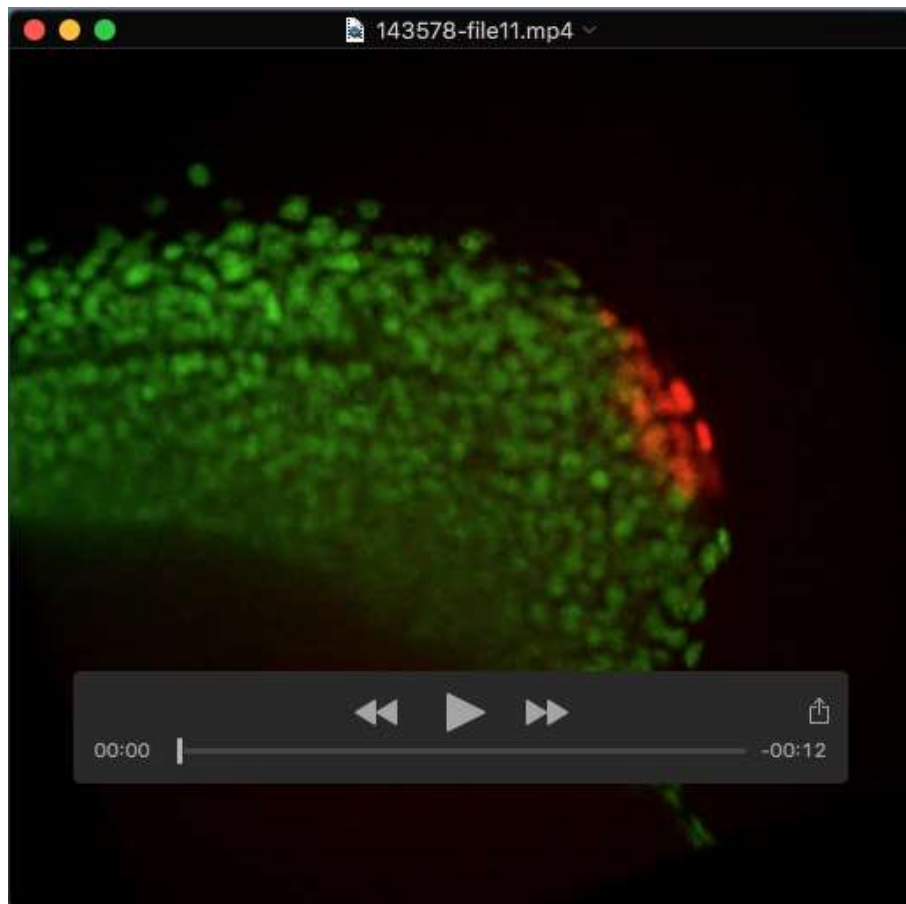
Movie 7. Cropped version of movie 6, focusing on the cell of interest.



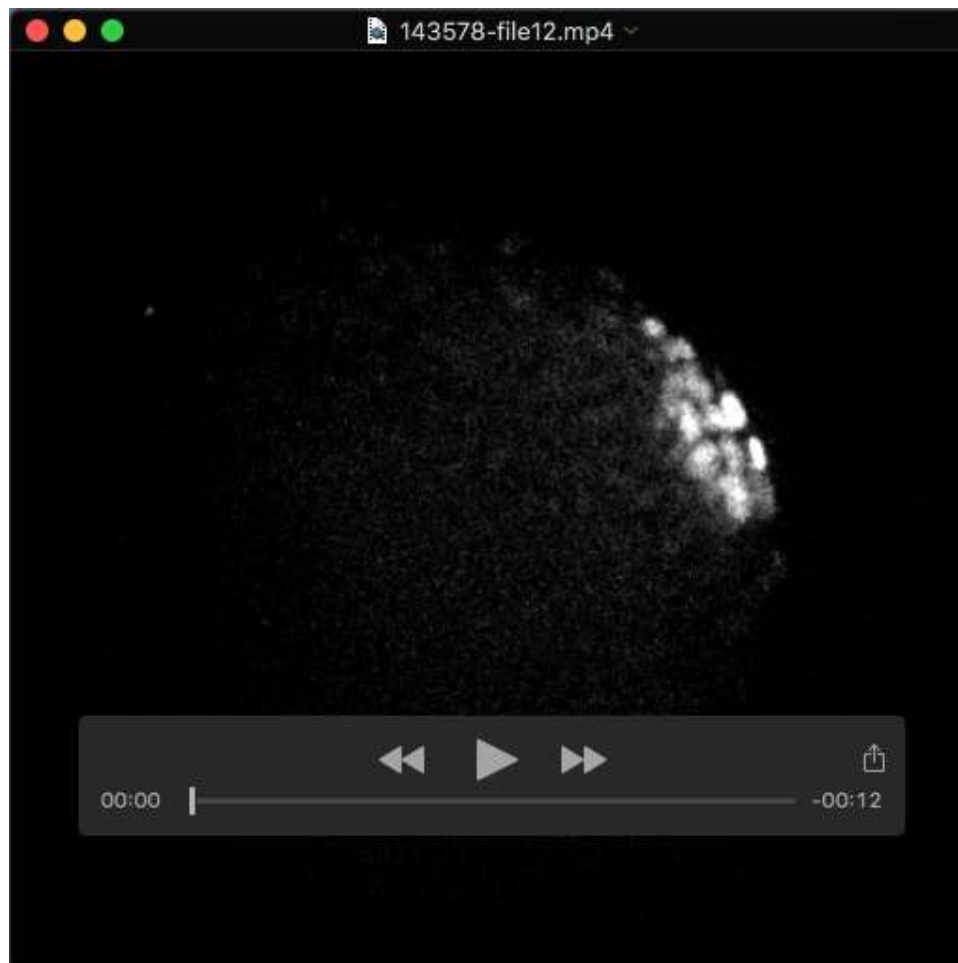
Movie 8. Time lapse movie of photoconverted cells in a wildtype tailbud (merged) A movie of wildtype photoconverted red tailbud cell with Z projection from 5 μ m Z-stacks merged with a projection of nonconverted cells in green. The embryo was treated with DMSO (vehicle). Images were acquired every 5 minutes for 5 hours. (5 frames per second).



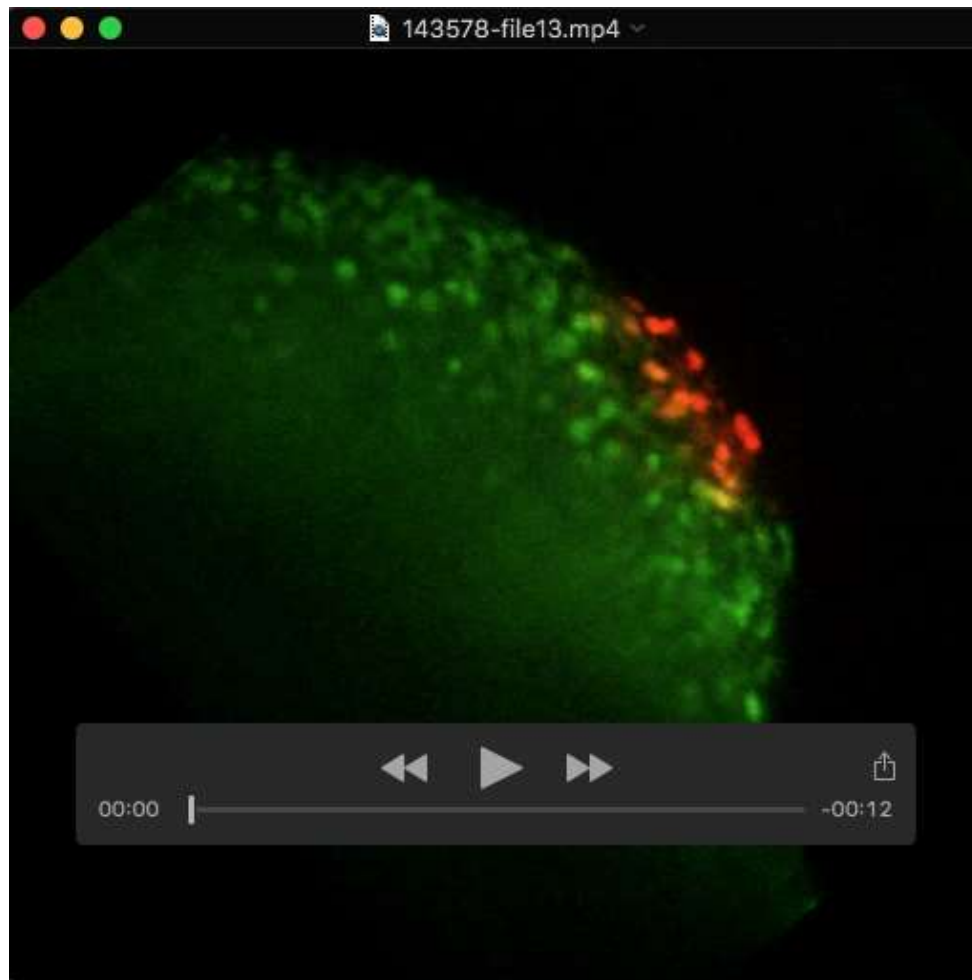
Movie 9. Time lapse movie of photoconverted cells in a wildtype tailbud (photoconverted cells only) A movie of wildtype photoconverted tailbud cell with Z projection from 5 μ m Z-stacks. The embryo was treated with DMSO (vehicle). Images were acquired every 5 minutes for 5 hours. (5 frames per second).



Movie 10. Time lapse movie of photoconverted *tbx16* overexpressed progenitors in the tailbud (merged) A movie of HS:*tbx16* photoconverted tailbud cells with Z projection from 5 μ m Z-stacks merged with unconverted green field projected plane. The embryo was treated with DMSO (vehicle). Images were acquired every 5 minutes for 5 hours. (5 frames per second).



Movie 11. Time lapse movie of photoconverted *tbx16* overexpressed progenitors in the tailbud (photoconverted cells only) A movie of DMSO treated HS:*tbx16* photoconverted tailbud cells with Z projection from 5 μ m Z-stacks. Images were acquired every 5 minutes for 5 hours. (5 frames per second).

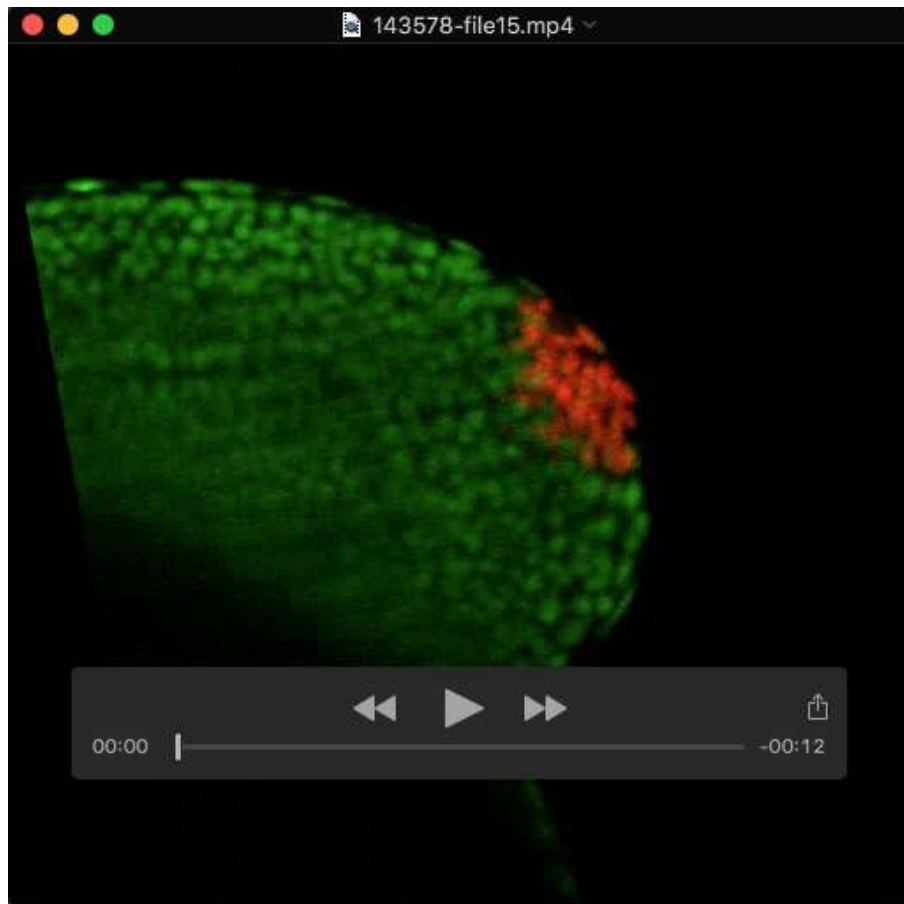


Movie 12. Time lapse of photoconverted FGF inhibited progenitors in the tailbud (merged)

Time lapse movie of SU5402 treated photoconverted tailbud cells with Z projection from 5um Z-stacks merged with a projection of nonconverted cells in green. Images were acquired every 5 minutes for 5 hours. (5 frames per second).



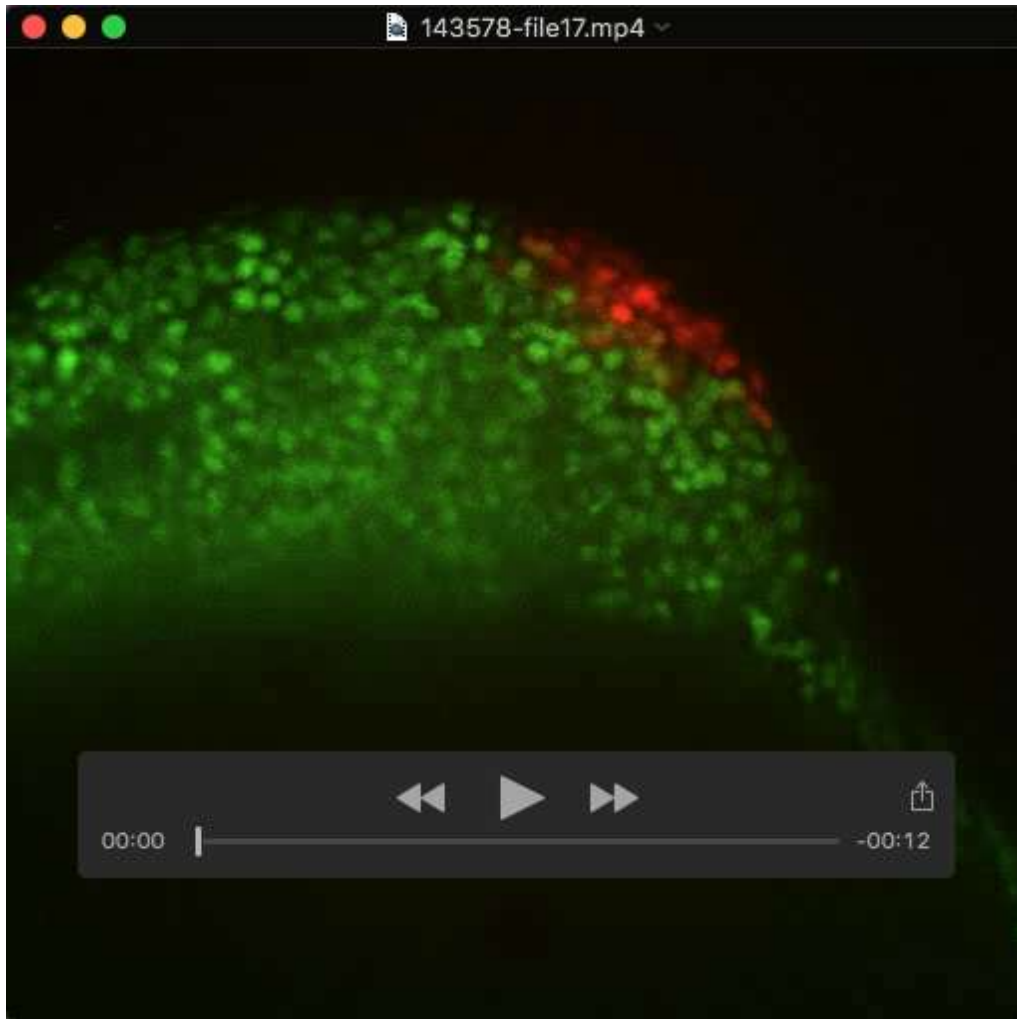
Movie 13. Time lapse of photoconverted FGF inhibited progenitors in the tailbud (photoconverted cells only) Time lapse movie of SU5402 treated photoconverted tailbud cells with Z projection from 5um Z-stacks. Images were acquired every 5 minutes for 5 hours. (5 frames per second).



Movie 14. Time lapse of photoconverted *tbx16* overexpressing progenitors in the SU5402 treated tailbud (merged) Time lapse movie of SU5402 treated photoconverted *HS:tbx16* tailbud cells with Z projection from 5um Z-stacks merged with a projection of unconverted green field plane. Images were acquired every 5 minutes for 5 hours. (5 frames per second).

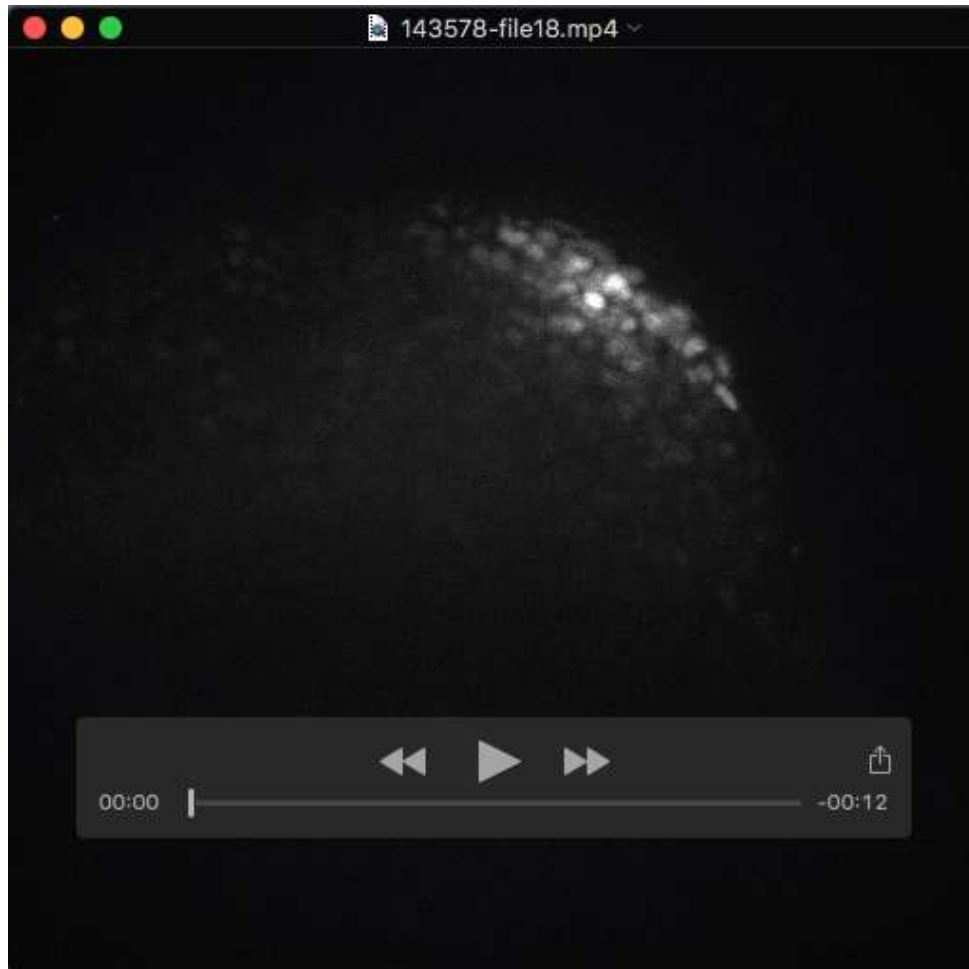


Movie 15. Time lapse of photoconverted *tbx16* overexpressing progenitors in the SU5402 treated tailbud (photoconverted cells only) Time lapse movie of SU5402 treated photoconverted nuclei of *HS:tbx16* tailbud cells with Z projection from 5um Z-stacks. Images were acquired every 5 minutes for 5 hours. (5 frames per second).



Movie 16. Time lapse of photoconverted FGF overactivating progenitors in the tailbud

(merged) Time lapse movie of DMSO treated photoconverted *HS:caFGFr1* tailbud cells with Z projection from 5 μ m Z-stacks merged with a projection of unconverted nuclei in green. Images were acquired every 5 minutes for 5 hours. (5 frames per second).



Movie 17. Time lapse of photoconverted FGF overactivating progenitors in the tailbud

(photoconverted cells only) Time lapse movie of DMSO treated photoconverted *HS:caFGFr1*

tailbud cells with Z projection from 5um Z-stacks. Images were acquired every 5 minutes for 5 hours. (5 frames per second).